A Volcano Rekindled: The Renewed Eruption of Mount St. Helens, 2004–2006
Edited by David R. Sherrod, William E. Scott, and Peter H. Stauffer
U.S. Geological Survey Professional Paper 1750, 2008

Chapter 31

Magmatic Conditions and Processes in the Storage Zone of the 2004–2006 Mount St. Helens Dacite

By Malcolm J. Rutherford[1] and Joseph D. Devine III[1]

Abstract

The 2004–6 eruption of Mount St. Helens produced dacite that contains 40–50 volume percent phenocrysts of plagioclase, amphibole, low-Ca pyroxene, magnetite, and ilmenite in a groundmass that is nearly totally crystallized. Phenocrysts of amphibole and pyroxene range from 3 to 5 mm long and are cyclically zoned, with one to three alternations of Fe- and Al-rich to Mg- and Si-rich layers showing little indication of phenocryst dissolution between zones. Similar-size plagioclase phenocrysts also contain several cyclic zones ranging between ~An_{68} and $An_{45–35}$. Textural evidence indicates that amphibole, pyroxene, and ilmenite began to crystallize before the most An-rich plagioclase. Magnetite and ilmenite phenocrysts are small (less than 100 μm), vary somewhat in composition from grain to grain, and are sporadically zoned. Magnetite-ilmenite pairs yield temperatures of equilibration ranging from 820ºC to 890ºC and f_{O_2} values of NNO +1 log unit. Magnetite compositions suggest that the 2004–6 magma was formed by mingling of magmas less than 5–8 weeks before eruption and that the magma last equilibrated within this temperature range. The amphibole phenocryst zoning involves approximately equal amounts of a pressure-sensitive Al-Tschermak molecular substitution and a temperature-sensitive edenite substitution in one cycle of growth. Hydrothermal experiments done on the natural dacite show that crystallization of the Fe- and Al-rich amphibole end member requires pressures of 200–300 MPa at temperatures of 900ºC, conditions approaching the upper temperature limit of amphibole stability. The dacitic magma crystallizes the An_{68} plagioclase when the pressure drops to 200 MPa at 900ºC. The magma must cool at this depth to produce a complete An_{68}–An_{40} plagioclase zone and a Mg-rich layer on the amphiboles before the magma is cycled back to a high pressure, when a new layer of Fe-rich amphibole is acquired. The amphibole crystallizing in the dacite experiments at less than 200 MPa is lower in aluminum than any compositions in the natural cyclically zoned phenocrysts. The outer rim on some 2004–6 amphibole phenocrysts appears to have formed in the 100–200 MPa range, as do some phenocrysts in the May 1980 dacite pumice. Plagioclase rims of An_{35} in the 2004–6 magmas indicate that phenocryst growth continued until the pressure decreased to 130 MPa and that ascent was slow until this depth. Magma then entered the conduit for a relatively rapid ascent to the surface as indicated by the very thin (less than 5 μm) decompression-induced rims on the amphibole phenocrysts.

Introduction

Mount St. Helens began to erupt in 2004 after 18 years of relatively shallow seismic activity and no eruptions, aside from a few gas explosions during 1989–91 (Mastin, 1994). The extrusion of a lava dome onto the 1980 crater floor during the 1980–86 time period marked the end of the eruption that began in 1980. However, seismic data collected during the past two decades (Moran, 1994; Moran and others, this volume, chap. 2) showed a continuous, moderate level of small-magnitude seismic activity directly beneath the volcano, particularly in the depth range of 3–12 km. In addition, there were significant increases in the level of seismic activity at 3–10-km depths in 1995, 1998, and 2002, suggesting the possibility that magma was ascending to a depth of 3 to 4 km beneath the crater floor at these times. In October 2004, following a brief period of steam-and-ash explosions, lava began erupting within the crater at the south margin of the 1980–86 lava dome, and a new lava dome has been building slowly from a steady eruption of dacite magma (Pallister and Thornber, 2005; Pallister and others, this volume, chap. 30).

[1] Geological Sciences Department, Brown University, 324 Brook Street, Providence, RI 02912

Samples of the new dome collected by the U.S. Geological Survey's Cascades Volcano Observatory (USGS–CVO) scientists in late October 2004 were very oxidized, reddish in color, and crystal rich; they are considered likely to be material left in the upper conduit from the 1986 eruption. Samples that were collected within 1–2 weeks of eruption in late November 2004 (SH304), in early January 2005 (SH305), and more recently are interpreted to be samples of new magma. Initially, it appeared that this new magma was simply remobilized 1980–86 magma, stored at some level, possibly at 3–4 km, as suggested by the seismic record. In support of this idea, the bulk compositions determined for the new lava (Pallister and others, this volume, chap. 30) show it to be only slightly more evolved than lava from the 1980–86 eruptions (65 rather than 63 weight percent SiO_2). However, some characteristics of the new lava samples pointed to a new magma source at depth, or at least reestablishment of the 1986 magma storage system at 7–12 km depth (Scandone and Malone, 1985). These characteristics included the presence of apparently stable amphibole phenocrysts, the presence of significant amounts of glass in many samples, and, most particularly, the identification of magnetite-ilmenite pairs yielding temperatures >900ºC (Pallister and Thornber, 2005; Rutherford and Devine, 2005). If the erupting magma had been stored at pressures less than 100 MPa (~4 km below the summit; Geschwind and Rutherford, 1995) then amphibole phenocrysts would have developed a thick reaction rim according to earlier work (Rutherford and Hill, 1993). Amphiboles in the 2004–6 magma generally lack evidence of any significant breakdown except for a thin (less than 5 μm) rim that is attributed to reaction with melt during ascent in the conduit (Rutherford and Devine, 2005). The greater than 900ºC temperatures from the 2004–6 oxides are higher than temperatures (860ºC) recorded from samples of the 1986 Mount St. Helens eruption (Rutherford and Hill, 1993), suggesting that hotter magma was involved in the 2004–6 eruptions.

The observations and the initial analyses of the 2004–6 lava samples (Pallister and Thornber, 2005) give rise to a number of questions that we have attempted to answer in this paper: (1) Where did phenocrysts in these magmas last equilibrate with the surrounding melt before entering the conduit and undergoing transport to the surface? This question can be addressed by studying the rim compositions of the phenocryst phases in the natural samples and by doing experiments designed to reproduce the phenocryst rim-melt equilibrium at different possible preeruption conditions. (2) Can the cyclic compositional zoning observed in all of the silicate phenocryst phases (plagioclase, amphibole and orthopyroxene) of the 2004–6 magma (Rutherford and Devine, 2005) be explained by crystallization of a dacite magma at different conditions, and, if so, what are those conditions? We have studied the phenocryst zoning analytically and experimentally to determine the range of conditions experienced by the magma over its preeruption crystallization history, and herein we use the data to create a model of magma dynamics within this subvolcanic system. (3) Finally, what are the preeruption conditions for the 2004–6 magma, and how do they compare with those determined for the 1980–86 magma samples (Rutherford and others, 1985; Rutherford and Devine, 1988)? What are the possible reasons for any differences observed?

Analytical and Experimental Methods

Samples of the new 2004–6 Mount St. Helens dacite dome were supplied by members of the USGS–CVO staff shortly after it became possible to collect them. Polished thin sections were made for mineral-chemistry and textural investigations of the different samples, and crushed powders were made of some samples for use in hydrothermal experiments. The phases in the natural samples were analyzed using a CAMECA SX100 microprobe for the crystalline phases and a CAMECA Camebax microprobe for glasses. Analytical methods used are identical to those of Rutherford and Devine (2003). Amphibole cation proportions were calculated using the method of Holland and Blundy (1994). The method of Cosca and others (1991) was used to calculate amphibole stoichiometry on the basis of 13 cations (Si, Al, Fe, Mg, Mn, and Ti) and to estimate ferric iron contents.

Experiments were performed on sample SH305-1 (erupted in November 2004), which was crushed to form a mixture of matrix and small (less than 0.2 mm) phenocryst fragments. This crushed sample was used in hydrothermal melting experiments and to create a glass-rich starting material for use in crystallization experiments. Melting and crystallization experiments were done in adjacent sealed tubes. The objective was to reversibly create new phenocryst growth under controlled conditions of pressure, temperature, and oxygen fugacity (P, T, and f_{O_2}). All of the experiments were done with $P_{H_2O} = P_{total}$ using previously described methods. The textural data indicate that amphibole crystallized before plagioclase in the 2004–6 magma, and this requires that the melt contain at least 4 weight percent dissolved H_2O (Merzbacher and Eggler, 1984) at this early stage of crystallization. With additional crystallization (primarily plagioclase and orthopyroxene), the melt would have rapidly approached water saturation for total pressures less than 300 MPa. The possibility that the 2004–6 magma initially contained some dissolved CO_2 cannot be ruled out, however, and is considered in the discussion.

Petrology of the 2004–2006 Dacite

General Petrology

The 2004–6 Mount St. Helens dacite is macroscopically similar to the material erupted in 1980–86. It is a crystal-rich dacite (~45 volume percent phenocrysts on a bubble-free basis) with phenocrysts of plagioclase, orthopyroxene, amphibole, Ti-magnetite, and ilmenite in a groundmass that is nearly totally crystallized in most of the samples (fig. 1;

Pallister and Thornber, 2005; Rutherford and Devine, 2005). Phenocrysts range up to 6 mm across and sporadically show some preferred orientation owing to magma flow. The groundmass and phenocryst assemblages are the same, except that amphibole is lacking in the groundmass and, instead, there is Ca-rich pyroxene and minor cristobalite and quartz. The bulk compositions of the 2004–6 magma samples have been remarkably uniform at 65 weight percent SiO_2 throughout the eruption (Pallister and others, this volume, chap. 30). The erupting magma resembles the magma that erupted in 1980–86 in that it contains several volume percent (fragments and crystal clots) of "gabbroic" material that is rich in plagioclase, pyroxenes, and amphibole (Heliker, 1995). As in the earlier eruption, a few of the inclusions in the 2004–6 samples contain interstitial melt (glass) that appears to represent partial melting, but many inclusions do not contain a glass phase. The smallest inclusions are difficult to distinguish macroscopically from phenocryst clots, but their amphibole differs from the phenocrysts compositionally and generally is not chemically zoned. Additionally, Ca-rich pyroxene commonly is associated with amphibole in the inclusions (Rutherford and Devine, 2005).

Plagioclase

The plagioclase phenocrysts in the Mount St. Helens 2004–6 magma are euhedral, complexly zoned crystals (fig. 1) as large as 5 mm in diameter, although most are less than 3 mm. These phenocrysts have a complex core-to-rim cyclic zoning easily observable in backscattered electron (BSE) images (fig. 2). The composition of the outer plagioclase rim ranges from An_{60} to An_{35}, but the great majority of the rims are relatively albite rich ($An_{30–35}$). Core compositions of the plagioclase phenocrysts range up to An_{68}. Plots of composition versus distance (rim to rim) across typical phenocrysts in the 2004–6 lava are shown in figure 2, and the compositions of a typical core and rim are given in table 1. Most boundaries between compositional zones are parallel to growth faces, with relatively little evidence of resorption involved in the zoning reversals (fig. 2). However, some resorption did occur during the plagioclase growth history, and 5 to 10 volume percent of the phenocrysts, including both small and large crystals, have a strongly sieved core with a relatively thin rim of clear plagioclase. A similar population of sieve-cored plagioclase phenocrysts was also observed in 1980–86 lava (Rutherford and others, 1985). Another characteristic of the plagioclase phenocrysts in the new lava is the relatively common presence of included crystals of amphibole, orthopyroxene, and Ti-magnetite, in decreasing order of abundance, particularly in the outer half of the phenocryst.

Amphibole

Amphibole phenocrysts in the Mount St. Helens dacite are euhedral, mostly 1–3 mm long but infrequently up to 5 mm in length, and commonly exhibit an internal cyclic compositional zoning parallel to growth faces (fig. 3). Petrographic examination shows some variability in amphiboles from samples erupted at different times during the 2004–6 eruption, particularly different amounts of opacitization due to variable syneruptive oxidation (Garcia and Jacobson, 1979; Rutherford and Hill, 1993) or decompression-induced rim development. The outer margins of some amphiboles appear somewhat rounded and possibly eroded or abraded (fig. 3*C*); whereas evidence for rounding or dissolution at internal zone boundaries is inconclusive (fig. 3). Inclusions in amphiboles are relatively uncommon compared to plagioclase phenocrysts, but magnetite and sulfide inclusions do occur. Larger inclu-

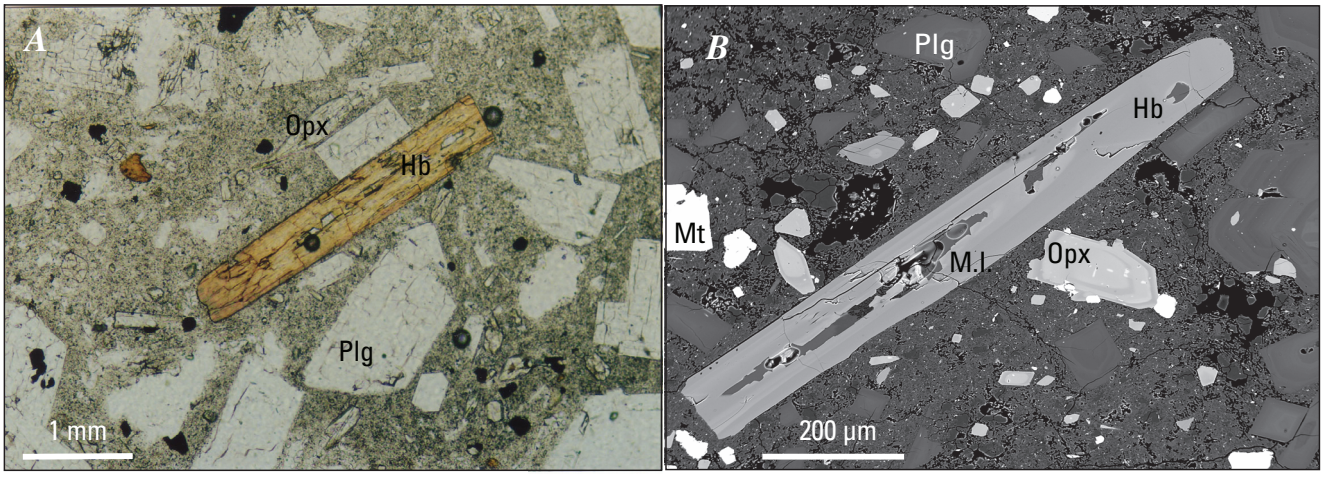

Figure 1. Photomicrographs showing thin section of typical Mount St Helens dacite assemblage. Phenocryst phases are plagioclase (Plg), amphibole (Hb), low-Ca pyroxene (Opx), all with obvious cyclic zoning, and magnetite (Mt); ilmenite is other phenocryst, not shown. Groundmass is largely crystallized and slightly vesicular. *A*, Plane-polarized transmitted light. *B*, Backscattered electron image. M.I., melt inclusion.

Table 1. Compositions of representative natural plagioclase and orthopyroxene phenocrysts in dacite erupted at Mount St. Helens, Washington, 2004–2006.

[Chemical analyses determined by electron microprobe at Brown University, Providence, R.I.; J.D. Devine, analyst. Compositions in weight percent; all Fe as FeO in pyroxene and as Fe_2O_3 in plagioclase. Magnesium number, Mg# = (Mg×100)/(Mg+(Fe^{2+} in octahedral site)).]

Plagioclase phenocrysts						
Sample No.---	**SH304c**	**SH304r**	**SH305c**	**SH305r**	**SH323r**	**SH323c**
SiO_2	53.54	60.19	52.16	58.69	58.46	51.86
Al_2O_3	29.56	25.16	29.86	26.73	26.40	30.81
Fe_2O_3	0.30	0.24	0.59	0.33	0.32	0.63
CaO	12.21	6.71	13.44	8.04	7.91	13.54
Na_2O	4.33	6.85	3.31	6.33	6.46	3.37
K_2O	0.11	0.25	0.17	0.25	0.24	0.08
Total	100.05	99.40	99.53	100.37	99.79	100.29
An content	60	35	69	40	39	68
Orthopyroxene phenocrysts						
Sample No.---	**SH304 Px1**	**SH304 Px2**	**SH305 Px1**	**SH305 Px2**	**SH323 Opx 1**	**SH323 Opx 2**
SiO_2	52.60	52.56	52.17	53.45	52.14	53.09
TiO_2	0.22	0.13	0.17	0.12	0.21	0.29
Al_2O_3	1.56	0.54	0.44	0.56	1.37	1.74
FeO	21.07	23.50	23.28	20.47	22.60	16.97
MgO	22.30	20.80	20.85	23.65	20.40	25.23
CaO	1.16	1.15	1.21	0.86	1.20	0.99
MnO	0.70	0.69	0.63	0.71	0.69	0.41
Cr_2O_3	0.00	0.01	0.02	0.01	0.01	0.06
Total	99.61	99.38	98.77	99.83	98.62	99.78
Mg#	63	60	60	63.5	61	64

sions in amphibole are generally multicrystalline and appear to represent trapped melts that have crystallized in what appears to have been a hollow-cored crystal (figs. 1, 3*A*–*C*). The amphiboles that occur in gabbroic inclusions are commonly not in contact with glass, except on the inclusion margins. Amphibole crystals in these inclusions are also generally anhedral, do not show cyclic compositional zoning, and are low in Al_2O_3 (8–11 weight percent) compared to the phenocrysts. Some isolated crystals in the dacite magma have similar characteristics.

The cyclic internal zoning present in the majority of amphibole phenocrysts in the 2004–6 Mount St. Helens lava is present in even the smallest (~100 μm) phenocrysts and is observable optically, as well as in BSE images. This zoning tends to begin with a bright BSE zone in the center of a phenocryst, involves one or two cycles of alternating bright-dark zoning, and ends with a dark, low-FeO zone adjacent to the groundmass (fig. 3). A similar zoning occurs in the amphiboles from the 1986 lava dome (fig. 3*D*), although the outer rim in these samples is intermediate to Fe-rich rather than Mg-rich. The Mg# (Mg/(Mg+Fe^{2+})) and ^{VI}Al profiles across representative amphibole phenocrysts are shown in figure 3, and compositions at points across typical cycles of amphibole growth are given in table 2.

The cyclic compositional zoning in the Mount St. Helens amphiboles involves Fe-, Al-, Na-, and K-enriched bright zones (BSE images) that alternate with, and grade into, Mg- and Si-rich dark BSE zones (figs. 3, 4). The cation substitutions involved in this zoning are similar to those observed in phenocrysts from the 1995–2002 Soufrière Hills andesite erupted on Montserrat (Rutherford and Devine, 2003) and in Fish Canyon latite (Bachmann and Dungan, 2002), but they differ in one significant aspect. A pressure-sensitive Al-Tschermak substitution was not inferred for either the Soufrière Hills or the

Fish Canyon amphibole zoning. In contrast, phenocrysts in the 2004–6 Mount St. Helens lava are marked by compositional variations that are ~50 mol percent Al-Tschermak substitution (^{M}(Mg, Fe) + ^{T}Si = ^{M}Al + ^{T}Al; fig. 5*A*), with the remaining change in ^{T}Al attributed to the temperature-dependent edenite (^{T}Si + ^{A}vacancy = ^{T}Al + ^{A}(Na+K)) and Ti-Tschermak exchanges (2^{T}Si + ^{M}Mn = 2^{T}Al + ^{M}Ti), as shown in figures 5*B* and 5*C*. In going from the Fe-rich to the Mg-rich zones, the decrease in Fe appears to be completely balanced by the increase in Mg in the octahedral position (fig. 6), as was found to be the case in previous studies (Bachmann and Dungan, 2002; Rutherford and Devine, 2003). In other words, the increase in ^{VI}Al in the amphibole structure is accompanied by an increase in Fe^{2+} at the expense of Mg^{2+} in the octahedral site (fig. 3).

One potentially important aspect of the amphibole phenocryst zoning in the 2004–6 Mount St. Helens magma is illustrated by the zoning in sample SH323 (fig. 7). Most amphibole phenocrysts in this sample have, in contrast to 2004–6 magma erupted earlier, a relatively bright (Fe-rich) rim, but the Al_2O_3 content is low and the SiO_2 content (fig. 4) is relatively high in this layer. Analytical electron-microprobe traverses across such phenocrysts show that the fluorine (F) content increases significantly over a distance of 20–40 μm at the phenocryst margin as Si increases and Al decreases. The core of the amphibole phenocryst contains 960±200 ppm F; the very outer margin of the phenocryst contains as much as 7,700 ppm (fig. 7*C*; table 2). A similar increase in F and Si was noted where the rim-to-rim analytical profile passed close to a melt channel in the phenocryst. Another, possibly related, observation is that the amphiboles in the gabbroic inclusions also are low in octahedral as well as total Al and Si relative to the cyclically zoned phenocrysts, and they are somewhat enriched in F (2,500 ppm) relative to the cyclically zoned phenocrysts (average of 900 ppm F). The presence of a thin, decompression-induced reaction rim at the contact of these phenocrysts with the groundmass indicates that the fluorine enrichment occurs before the final magma ascent and decompression. One possible explanation of the fluorine zoning is that these crystals and crystal rims represent a partial recrystallization of amphiboles at conditions of low *P* and high activity of SiO_2 just outside the OH-bearing amphibole stability field. Similar overgrowths are observed on amphibole phenocrysts

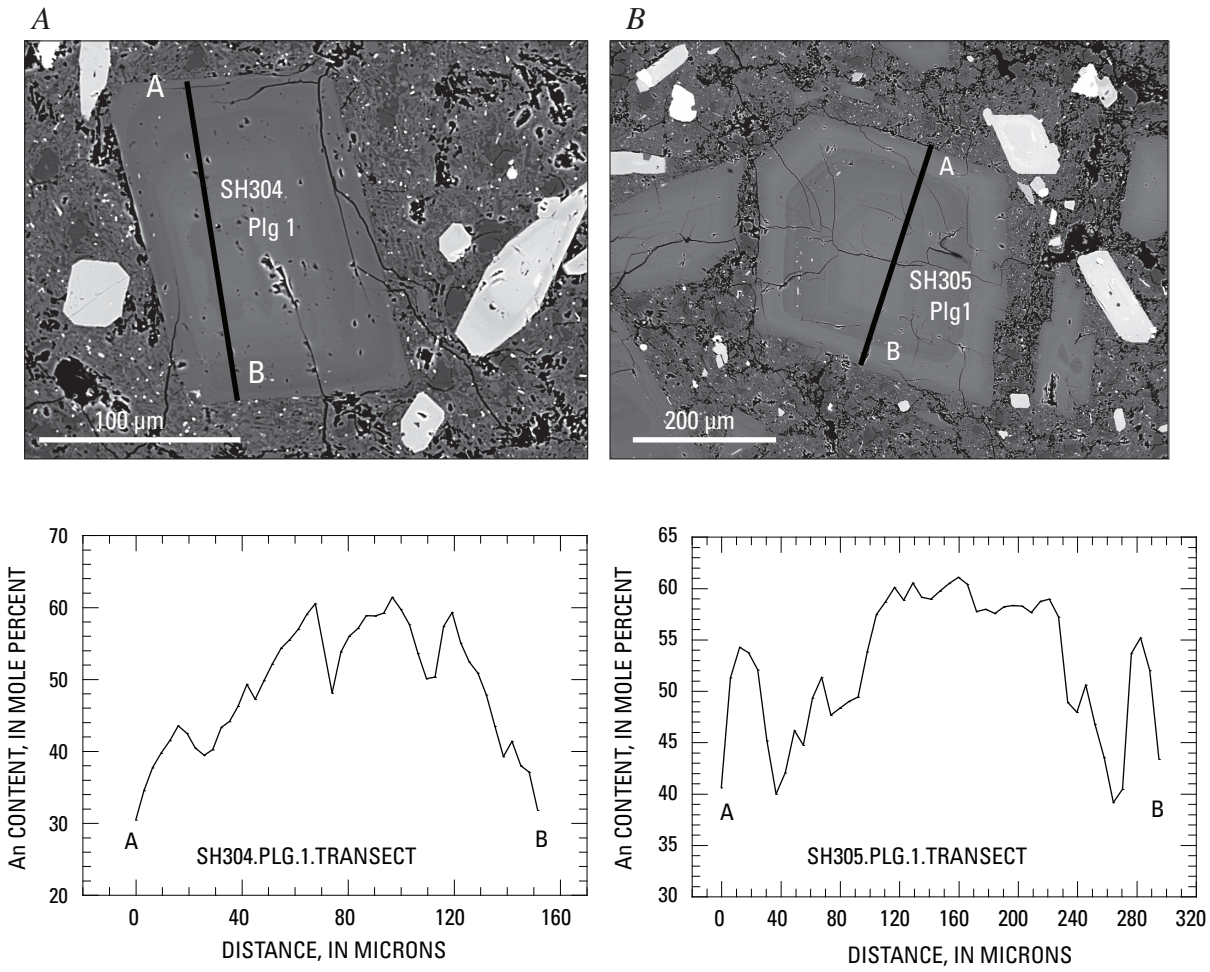

Figure 2. Backscattered electron images from thin section of Mount St. Helens lava, showing typical plagioclase phenocryst of 2004–6 lava. Images show cycles of light (Ca-rich) and dark (Na-rich) phenocryst growth; accompanying graphs depict An concentrations along the A–B profiles. *A*, Plagioclase in sample SH304. *B*, Plagioclase in sample SH305.

Table 2. Representative natural amphibole compositions in dacite erupted at Mount St. Helens, Washington, 2004–2006.

[Chemical analyses determined by electron microprobe at Brown University, Providence, R.I.; J.D. Devine, analyst. Compositions in weight percent; all Fe as FeO; n.d., not determined. Structure formula calculated after Holland and Blundy (1994). Magnesium number, Mg# = (Mg×100)/(Mg+(Fe^{2+} in Y site)).]

Sample No.--- Site---------- Character-----	SH304-1-2 Hb7 rim Hi-Mg	SH304-1 Hb7 interior Med.-Al	SH304-1 Hb7 core Hi-Al	SH305a Hb rim Low-Al	SH305b Core Hi-Al
			Major-element analyses, weight percent		
SiO_2	44.80	42.86	40.97	43.51	40.40
TiO_2	1.95	2.41	2.56	2.72	2.40
Al_2O_3	11.40	13.09	14.30	11.97	14.86
FeO	12.30	12.90	15.31	11.99	16.05
MgO	15.43	13.92	11.82	14.97	10.54
CaO	11.29	10.67	10.74	11.58	11.39
Na_2O	1.98	2.37	2.39	2.39	2.26
K_2O	0.20	0.30	0.31	0.32	0.35
MnO	0.16	0.15	0.21	0.10	0.16
Cr_2O_3	0.02	0.01	0.01	0.00	0.00
Total	99.51	98.92	98.61	99.55	98.41
			Cation abundance in structure formula		
Si	6.305	6.128	5.942	6.170	5.923
^{IV}Al	1.695	1.872	2.058	1.830	2.077
Ti	0.206	0.259	0.279	0.290	0.265
^{VI}Al	0.196	0.333	0.386	0.171	0.490
Cr	0.007	0.001	0.008	0.000	0.000
Fe^{3+}	0.893	0.802	0.842	0.725	0.681
Fe^{2+}(Y)	0.468	0.639	0.938	0.649	1.261
Mg	3.237	2.966	2.555	3.164	2.303
Ca	1.702	1.634	1.669	1.760	1.809
Fe^{2+}(X)	0.087	0.101	0.077	0.047	0.026
Mn	0.019	0.018	0.026	0.012	0.020
Na	0.541	0.657	0.673	0.676	0.642
K	0.036	0.055	0.057	0.058	0.065
Mg#	87.37	82.27	73.14	82.98	64.62
$Fe^{3+}/\Sigma Fe$	0.617	0.520	0.453	0.510	0.346

erupted later in 2005 (SH324) and in 2006 (SH328), when the magma mass-eruption rate was also relatively low (Pallister and others, this volume, chap. 30).

Low-Ca Pyroxene (Orthopyroxene)

The orthopyroxene phenocrysts present in the 2004–6 magma are commonly cyclically zoned parallel to growth surfaces, similar to the zoning observed in amphibole. Examples where the zoning stands out as alternating light and dark bands are present in figures 1*B*, 3*A*, and 3*B*. Compositional profiles across a typical zoned phenocryst are shown in figure 8 for the pyroxene that is present in figure 1*B*. Like the amphibole, pyroxene phenocrysts can have as many as four cycles of light and dark zones rich in Fe and Mg, respectively, but many have only two. The smaller number of cycles visible in BSE and compositional profiles across orthopyroxene phenocrysts might be related to their smaller size, although some 100-μm-diameter crystals have as many as three light-dark growth cycles (fig. 3*A*). The trend from cycle to cycle is similar in both amphibole and orthopyroxene, in that the transition from dark, Mg-rich to bright, Fe-rich bands is sharp, whereas the bright to dark transition is gradational (figs. 1, 3). This similar-

Table 2. Representative natural amphibole compositions in dacite erupted at Mount St. Helens, Washington, 2004–2006.—Continued

[Chemical analyses determined by electron microprobe at Brown University, Providence, R.I.; J.D. Devine, analyst. Compositions in weight percent; all Fe as FeO; n.d., not determined. Structure formula calculated after Holland and Blundy (1994). Magnesium number, Mg# = (Mg×100)/(Mg+(Fe^{2+} in Y site)).]

Sample No.------	SH308-1	SH308-1	SH323	SH323	SH323
Site----------	#1 rim	#3 core	Rim	Near rim	27 core
Character--------	Low-Al	Med.-Al	Low-Al	Med.-Al	Hi-Al
			Major-element analyses, weight percent		
SiO_2	43.89	41.53	43.88	41.15	42.08
TiO_2	2.43	2.27	2.56	2.88	2.22
Al_2O_3	11.38	13.31	10.25	13.88	14.11
FeO	12.48	14.97	14.69	14.65	14.79
MgO	15.15	12.12	13.69	12.23	12.65
CaO	10.71	11.02	11.07	11.40	10.74
Na_2O	2.32	2.25	2.46	2.96	2.83
K_2O	0.23	0.35	0.31	0.27	0.27
MnO	0.08	0.23	0.21	0.14	0.23
Cr_2O_3	0.06	0.01	0.01	0.00	0.00
F	n.d.	n.d.	0.77	0.102	0.096
Total	98.73	98.06	99.90	99.66	100.02
			Cation abundance in structure formula		
Si	6.251	6.054	6.375	5.957	6.017
^{IV}Al	1.749	1.946	1.625	2.043	1.983
Ti	0.260	0.249	0.280	0.314	0.239
^{VI}Al	0.162	0.341	0.130	0.325	0.395
Cr	0.007	0.001	0.001	0.000	0.000
Fe^{3+}	0.827	0.807	0.716	0.584	0.777
Fe^{2+}(Y)	0.528	0.968	0.909	1.139	0.893
Mg	3.216	2.633	2.964	2.639	2.696
Ca	1.634	1.721	1.723	1.768	1.645
Fe^{2+}(X)	0.131	0.049	0.160	0.051	0.098
Mn	0.010	0.028	0.026	0.017	0.028
Na	0.641	0.636	0.693	0.831	0.785
K	0.042	0.065	0.057	0.050	0.049
Mg#	85.89	73.12	76.53	69.86	75.12
$Fe^{3+}/\Sigma Fe$	0.556	0.442	0.401	0.329	0.440

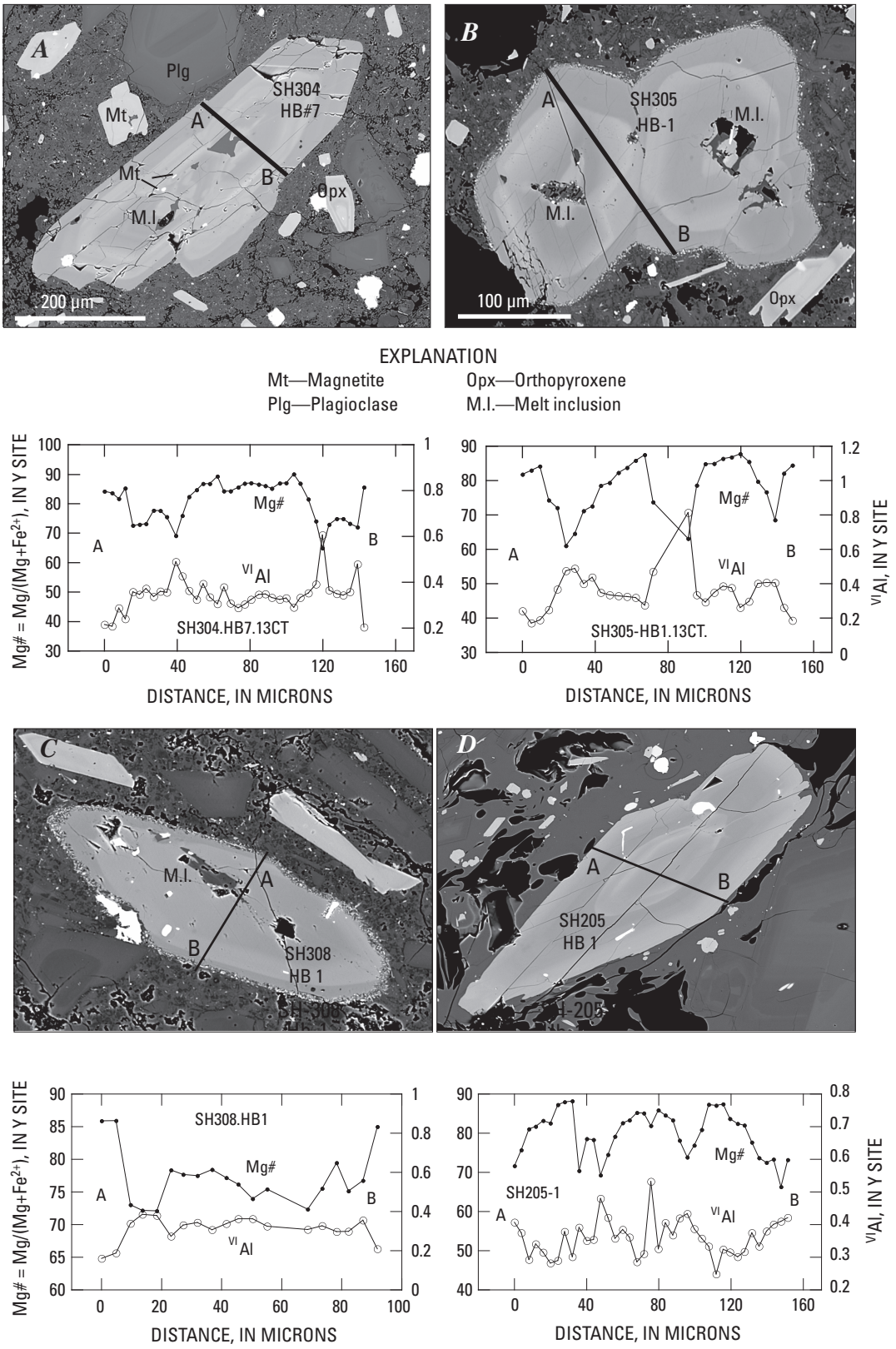

Figure 3. Backscattered electron images of typical amphibole and orthopyroxene phenocrysts; accompanying graphs show compositional profiles along lines A–B in each image. Note growth cycles of alternating Fe-rich (bright) and Mg-rich (dark) zoning. Compositional profiles show the Fe-rich zones are also rich in octahedral-coordinated Al (^{VI}Al). *A*, Sample SH304. *B*, Sample SH305. *C*, Sample SH308. *D*, Sample SH205 from 1986 dacite lava dome.

ity in compositional zoning implies that the two minerals were co-crystallizing as *P–T* conditions in the magma went through a series of cycles. As in the amphibole, the Al and Ti concentrations in orthopyroxene are slightly higher in the Fe-rich zones, but the correlation is not strong (fig. 8). The lack of a correlation of Fe with Al in pyroxene is probably due in part to the fact that the Al_2O_3 content is low (0.5–1.5 weight percent). Analyses of representative pyroxene phenocrysts are given in table 1.

Fe-Ti Oxides

Subhedral to rounded Fe-Ti oxide crystals (<150 μm rim to rim) are present in all samples studied. Titanomagnetite phenocrysts in dome lavas characterized by relatively rapid volumetric extrusion rates (6.5 m^3/s; Pallister and others, this volume, chap. 30) are commonly homogeneous in composition from core to rim, although TiO_2 contents may vary

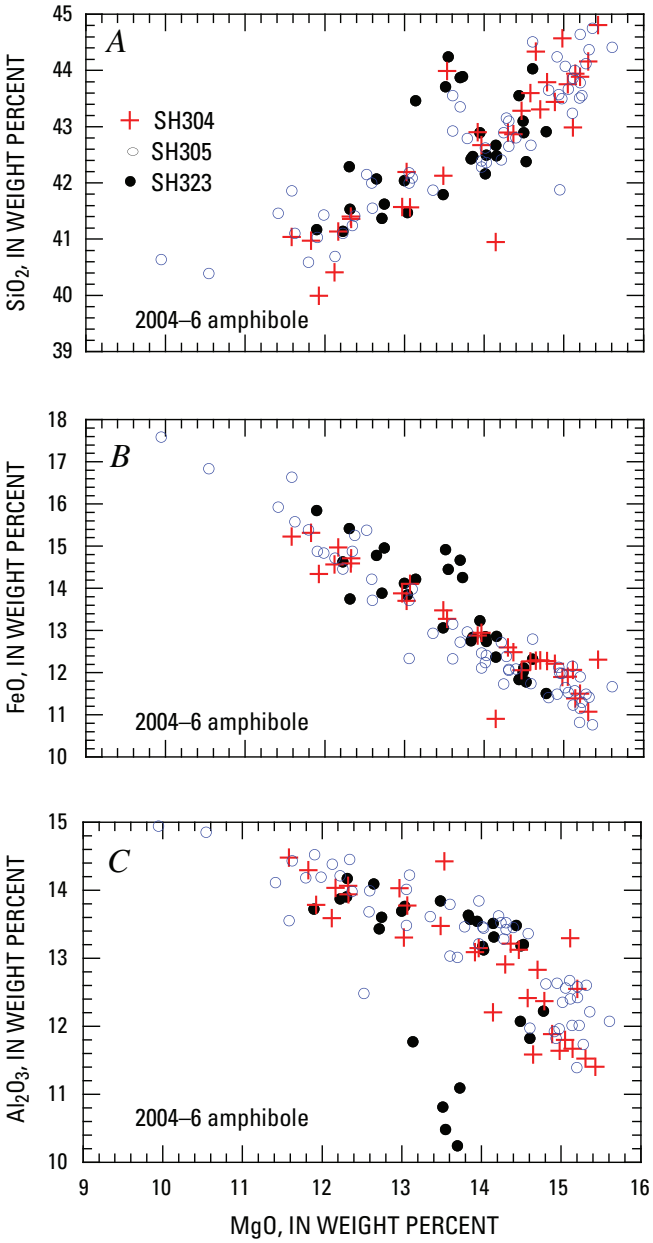

Figure 4. Chemical variation diagrams showing rim-to-rim compositional zoning in typical amphibole phenocrysts from three samples of the 2004–6 eruption. *A*, MgO vs. SiO_2. *B*, MgO vs. FeO. *C*, MgO vs. Al_2O_3. Crystal rims in SH323 (five points) with anomalously high SiO_2 (panel *A*) and low Al_2O_3 (panel *C*) are discussed elsewhere in the paper.

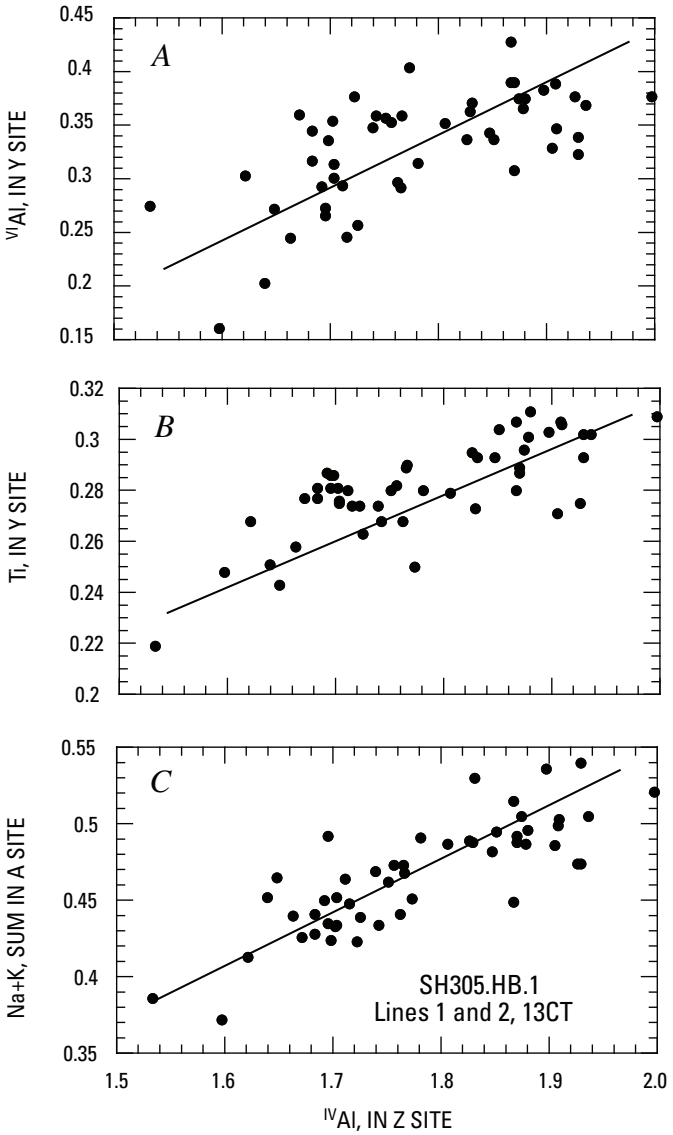

Figure 5. Plots showing position of chemical species in crystallographic sites versus tetrahedrally coordinated Al (^{IV}Al) in Z site for typical, cyclically zoned amphibole in lava samples from Mount St. Helens 2004–6 eruption. *A*, Octahedrally coordinated Al (^{VI}Al) in the Y site. *B*, Ti in the Y site. *C*, Sum of Na+K in the A site. Note that approximately equal amounts of the ^{IV}Al increase are balanced by increases in ^{VI}Al and the sum of Na and K.

substantially from grain to grain, even within the same hand sample (fig. 9). There is no apparent correlation between TiO_2 content and grain size (fig. 9). Lava samples characterized by relatively low volumetric extrusion rates have titanomagnetite crystals that contain lamellae of titanohematite that occur in trellis-like intergrowths with titanomagnetite that is higher in TiO_2 content than the presumed parent. Titanohematite grains in the groundmass of such oxidized samples impart a reddish color to the rocks.

Subhedral to anhedral ilmenite grains (typically less than 50 μm), though rare, are present in every sample. Many grains appear to be embayed to a greater or lesser extent. The TiO_2 contents of the ilmenite grains in rapidly extruded lavas are essentially bimodally distributed, with one group somewhat higher in TiO_2 (~44 weight percent) and lower in FeO* (~48 weight percent, all iron as FeO) than the other (TiO_2 ~42 weight percent; FeO* ~50 weight percent). Analyses of representative phenocrysts are included in table 3. Individual grains are essentially homogeneous in composition except for the outermost rim, which may be somewhat higher in TiO_2 than the cores. In some slowly extruded samples, near-surface oxidation processes have resulted in decomposition of the ilmenite and its replacement by veinlets of titanohematite, interspersed with rare small patches of a TiO_2 polymorph (greater than 83 weight percent TiO_2), likely rutile.

Rare ilmenite-titanomagnetite in-contact pairs are present in all samples examined. Concentration gradients for TiO_2 in titanomagnetite crystals in contact with ilmenite are commonly observed in these oxide pairs, with high TiO_2 adjacent to the ilmenite. Analyses of coexisting oxide pairs are given in table 3, together with the temperature and oxygen fugacity indicated by the coexisting compositions.

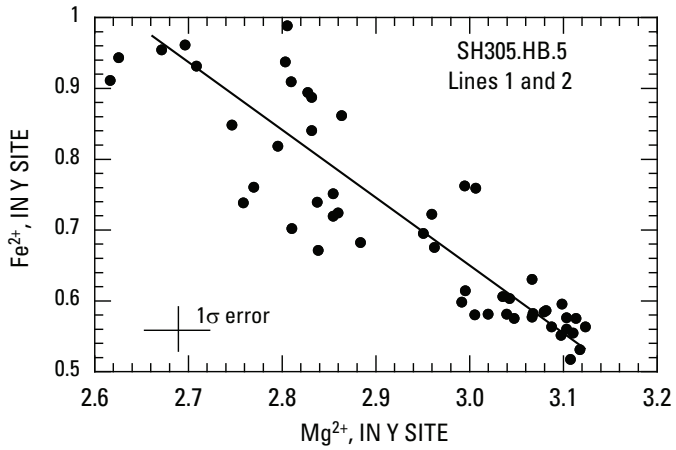

Figure 6. Plot of Mg^{2+} versus Fe^{2+} for the same amphibole phenocryst data plotted in figure 5, illustrating 1:1 correlation of Fe and Mg in the Y site of cyclically zoned 2004–2006 phenocrysts.

Preeruption Magma Conditions Inferred from the Phenocrysts

The compositions of the coexisting Fe-Ti oxides in the different samples of the 2004–6 Mount St. Helens dacite have been used to obtain estimates of temperature and f_{O_2} of the magma during the period of last magnetite-ilmenite equilibration. Methods of conversion are those described by Devine

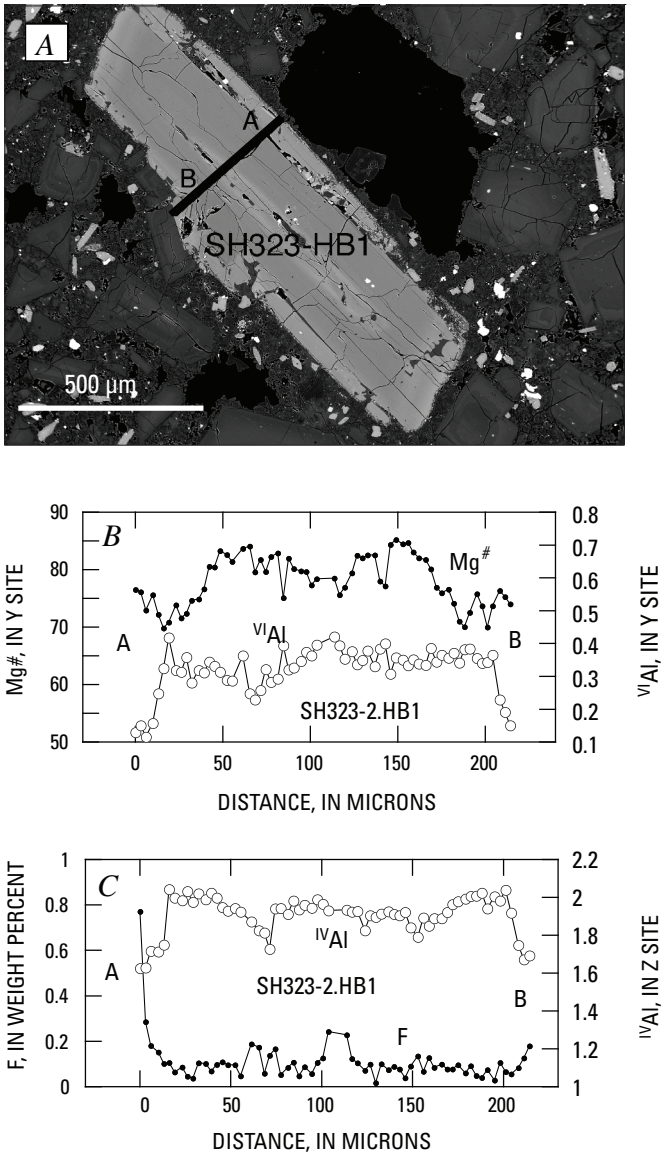

Figure 7. Typical amphibole phenocryst in sample SH323 erupted in September 2005 when the mass eruption rate had dropped to about 1 m^3/s (Pallister and others, this volume, chap. 30). *A*, Backscattered electron image showing compositional traverse as line A–B. *B*, *C*, Compositional traverses, showing presence of a rim less than 30 μm thick with low Al and Mg (panel *B*) and high F (panel *C*). Profile for SiO_2 across same phenocryst (fig. 4) shows the rim is also enriched in Si.

and others (2003) and utilize the algorithm of Andersen and Lindsley (1988) as amended by Andersen and others (1993). However, meaningful geothermometry based on analysis of ilmenite-titanomagnetite (two-oxide) pairs in these samples is hampered by the common presence of TiO_2 concentration gradients in the titanomagnetite grains, especially near the contact with ilmenite. Similar occurrences in the 1995–2003 Soufrière Hills volcano (Montserrat) andesite dome lavas were interpreted to be caused by replacement of the ilmenite grains by the in-contact encroaching titanomagnetite grain (Devine and others, 2003). The concentration gradients were interpreted as arising from submicron-scale mixtures of encroaching titanomagnetite upon islands of relict ilmenite. It was concluded in that case that temperature estimates based on analysis of the titanomagnetite crystal in the gradient zone (likely a two-phase mixture) were spurious. In some cases, two-oxide geothermometry calculations for the gradient zones yielded temperature estimates greater than 1,000ºC, far above the experimentally determined upper stability limit (855ºC) of the amphibole crystals observed to be stable in the natural magma (Rutherford and Devine, 2003). The two-oxide geothermometry calculations produced spurious results for zoned oxide pairs. Similar high-Ti magnetite zones adjacent to ilmenite in the Mount St. Helens 2004–6 magma are interpreted to give spurious temperature estimates for the same reasons.

In addition to using pairs of titanomagnetite and ilmenite (table 3), estimates of preeruptive magma temperatures also were attempted by analyzing the cores of large individual titanomagnetite and ilmenite grains in the 2004–6 lava samples. The titanomagnetite analyses in SH305 fall into three groups, with high, intermediate, and low TiO_2 contents (fig. 9). The range of TiO_2 contents observed in the titanomagnetite crystals might, in part, reflect incorporation of xenolithic material from the conduit walls. Temperature estimates based on the combined analytical transects range from 816ºC to 889ºC for sample SH305 and from 823ºC to 884ºC for sample SH315. A significant part of the variance in the estimates is due to the wide range of compositions observed in the respective phases. Temperature estimates based on analyses of titanomagnetite grains in the intermediate-TiO_2 group range from 823ºC to 846ºC when used in combination with the high-TiO_2 ilmenite; the range of temperature estimates is 854–875ºC when the low-TiO_2 ilmenite is used in the calculations. Oxygen fugacities generally are less than one log unit above the NNO synthetic buffer (range +0.6 to +1.2 log units) at the calculated temperatures in all cases.

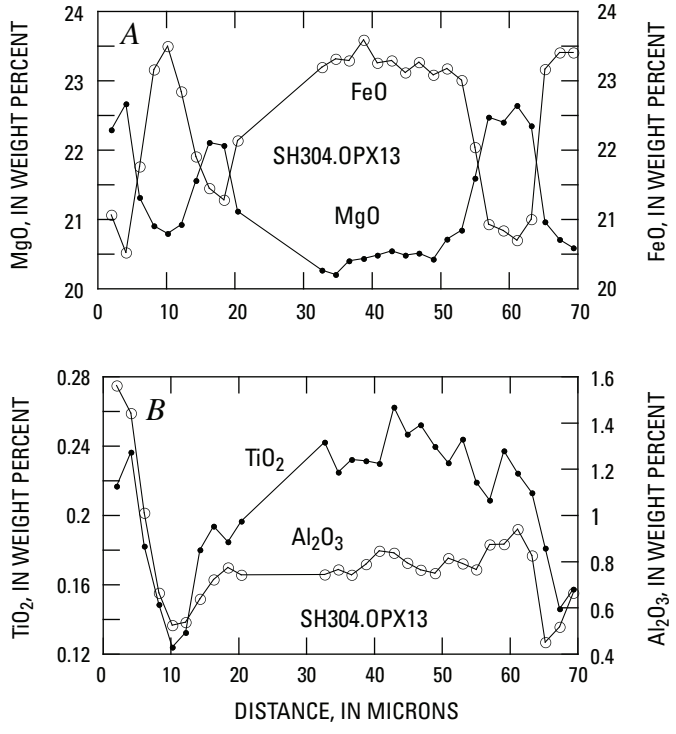

Figure 8. Compositional profiles (rim to rim) across typical zoned orthopyroxene in sample SH304 (phenocryst imaged in fig. 1*B*). Note tendency of Ti and Al to be correlated with Fe in the pyroxene growth cycles as they are in amphibole (figs. 5, 6). *A*, MgO and FeO. *B*, TiO_2 and Al_2O_3.

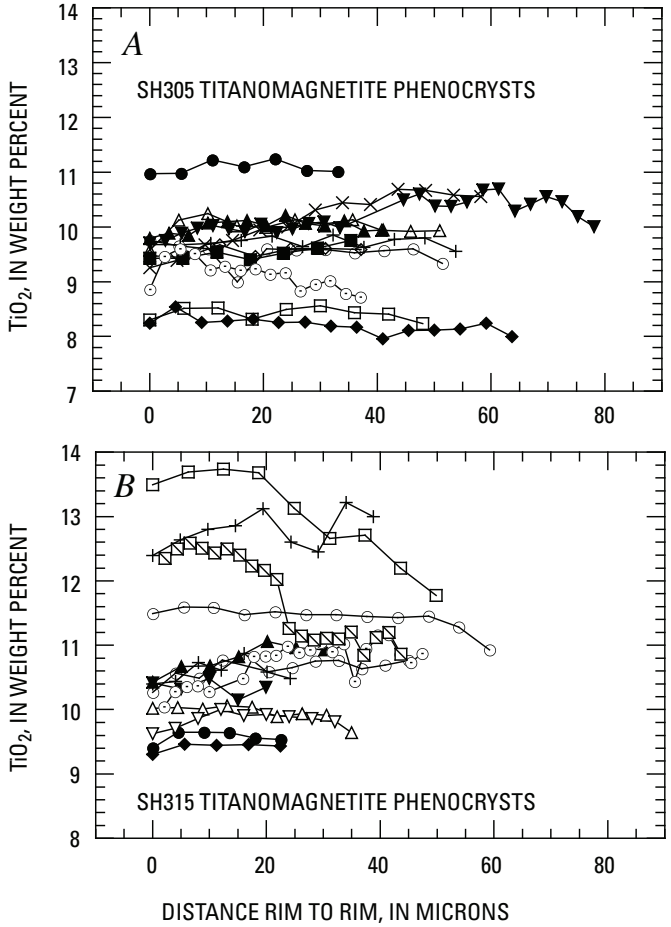

Figure 9. Composition (TiO_2) profiles across representative titanomagnetite phenocrysts in samples SH305 (*A*) and SH315 (*B*) from the 2004–6 eruption, showing range of relatively homogeneous crystals present.

Table 3. Chemical composition of ilmenite and titanomagnetite occurring as pairs, with calculated temperature and f_{O_2} of last equilibration geothermometry and oxygen geobarometry, Mount St. Helens, Washington, 2004–2006.

[Chemical analyses determined by electron microprobe at Brown University, Providence, R.I.; J.D. Devine, analyst. Compositions in weight percent; all Fe as FeO. Structural formula, temperature, and oxygen fugacity calculated after Devine and others (2003). Oxide phases abbreviated as follows: ILM, ilmenite; MT, magnetite.]

Sample No.----	**SH304-1b2**		**SH305-1-8**		**SH305-1-8**	
Date erupted--	**10/18/04**		**11/20/04**		**11/20/04**	
Relation--------	**Oxide pair in plag**		**Oxide pair in proximity**		**Oxide pair, small grains**	
Oxide	ILM	MT	ILM	MT	ILM	MT
FeO	51.39	82.85	49.94	80.67	50.34	74.88
TiO_2	42.98	8.54	44.02	11.13	44.36	12.73
Al_2O_3	0.21	2.33	0.17	1.79	0.21	1.74
Cr_2O_3	0.01	0.02	0.02	0.03	0	0.02
MgO	1.83	0.92	2.04	1.09	1.75	0.84
MnO	0.54	0.4	0.62	0.43	0.62	0.41
Total	96.96	95.06	96.82	95.15	97.29	90.63
Analyses	14	5	4	11	3	3
TºC	847		879		922	
$Log_{10} f_{O_2}$	−11.82		−11.10		−11.59	
ΔNNO	+1.16		+0.79		+0.50	
Sample No.----	**SH305-1-8**		**SH315-1a**		**SH315-1a**	
Date erupted---	**11/20/04**		**4/1/05**		**4/1/05**	
Relation--------	**Oxide pair in contact**		**Oxide pair in proximity**		**Oxide pair in proximity**	
Oxide	ILM	MT	ILM	MT	ILM	MT
FeO	51.90	78.65	49.24	82.63	51.27	82.29
TiO_2	41.75	13.77	45.07	9.57	43.22	7.86
Al_2O_3	0.22	1.48	0.14	1.47	0.16	2.80
Cr_2O_3	0.02	0.03	0.02	0.06	0.02	0.02
MgO	1.90	1.20	1.74	0.91	1.80	1.23
MnO	0.56	0.52	0.63	0.44	0.44	0.37
Total	96.35	95.65	96.84	95.09	96.91	94.57
Analyses	5	7	14	6	5	7
TºC	963		828		832	
$Log_{10} f_{O_2}$	−10.22		−12.57		−12.07	
ΔNNO	+0.70		+0.79		+1.21	

In spite of the difficulty of obtaining meaningful temperature estimates from in-contact Fe-Ti oxide pairs in the Mount St. Helens 2004–6 magma, the presence of the TiO_2 concentration gradients is evidence of a recent heating event (Nakamura, 1995; Venezky and Rutherford, 1999). However, the general lack of rim-to-core TiO_2 diffusion gradients in titanomagnetite phenocrysts suggests that heating of the crystals must have taken place some weeks before eruption, judging from experimental work on similar samples (Rutherford and Devine, 2003; Devine and others, 2003) and from diffusion data on Ti in magnetite (Venezky and Rutherford, 1999). It appears likely that the variability of TiO_2 contents in titanomagnetite is due in part to commingling of parcels of magma that experienced different *P–T* histories prior to eruption. This interpretation is consistent with observations of cyclic variations of amphibole and orthopyroxene chemistry described above.

Two other important intensive parameters that can occasionally be determined for a preeruption magma using phenocryst and melt compositions are the pressure (depth) and the P_{H_2O} (for example, Rutherford and others, 1985). The phenocryst assemblage in the 2004–6 magma suggests an intermediate depth (greater than 3.5–4 km) because the stability of

amphibole in a melt requires that the water content of the melt be at least equal to H_2O saturation at 100 MPa (Merzbacher and Eggler, 1984). The compositions of coexisting amphibole and plagioclase can also potentially yield both pressure and temperature information (Holland and Blundy, 1994), but the complex compositional zoning in both these phases makes it difficult to determine what amphibole coexists with a given plagioclase. In an attempt to circumvent this problem, the margins of amphibole crystals included in plagioclase were analyzed along with the immediately adjacent plagioclase for the 2004–6 magma samples. The results showed a complete range of amphibole compositions in contact with a given plagioclase and, thus, no decipherable indication of pressure or temperature. Similarly, the analysis of glassy melt inclusions in phenocrysts have yielded important data on the volatile content of the preeruption melt for other eruptions (for example, Rutherford and others, 1985; Wallace, 2005), but the relatively slow ascent and eruption of the 2004–6 dacite appears to have caused cracking and/or crystallization of almost all melt inclusions in the new Mount St. Helens magma. Analyses of 2004–6 samples indicate dissolved water contents less than 3 weight percent (J. Blundy, oral commun., 2006), and CO_2 below FTIR detection limits (less than 40 ppm).

The observation that amphibole crystallized before plagioclase in the 2004–6 samples indicates that this dacite contained at least 4 weight percent dissolved H_2O when the crystallinity was very low (less than 4–8 volume percent), as discussed above. This means that when the phenocryst content of the dacite reached the preeruption 40–50 volume percent as the result of decompression and/or cooling, the dissolved H_2O in the remaining melt would have almost doubled. In fact, the residual melt probably would have reached H_2O saturation where the storage-region pressure was less than 300 MPa. These arguments assume that all magma entering the magma storage zone was similar in composition, including dissolved volatiles. The fact that the erupted dacite has been uniform in composition and contains no mafic melt-bearing enclaves (Pallister and others, this volume, chap. 30) suggests that this assumption is justified.

Experimental Phase Equilibrium Constraints

In order to determine the *P–T* conditions where the compositions of the phenocrysts observed in the 2004 Mount St. Helens magma are stable, hydrothermal experiments were performed on a crushed powder of SH305. Experiments were done using water-saturated conditions, a decision justified by arguments presented in the previous section. Most experiments were at a log f_{O_2} close to NNO+1 because of the f_{O_2} conditions determined from the Fe-Ti oxide phenocrysts, but higher and lower oxidation states also were investigated using solid-state buffers. Sample and buffer were contained in Ag or Ag-Pd tubes. Details of the experiments are given in table 4, and the results are plotted in figure 10. The main objective of these experiments was to determine the composition of the amphibole and plagioclase that is stable (grows in experimental charges previously equilibrated at somewhat higher or lower P_{H_2O} and *T*) at each point in the range of *P–T* conditions where amphibole is stable in the magma. Our interest in the amphibole stability in this dacite magma stems from the observation that the main amphibole population appears to have crystallized at a range of conditions within the amphibole stability field prior to the final magma ascent to the surface. The final magma ascent is represented by the 0- to 5-μm-thick reaction rims that occur at the amphibole-melt contact (Rutherford and Devine, 2005).

As expected, the general hydrothermal phase equilibria of the 2004–6 dacite are similar to those determined for the slightly less evolved 1980 lava (63 versus 65 weight percent SiO_2). The amphibole stability field at the f_{O_2} conditions (NNO +1.0±0.5) of the many reconnaissance experiments is essentially unchanged by the composition difference, with the breakdown at 200 MPa occurring at 910±8ºC (fig. 10). Above 200 MPa, the reaction to form amphibole with decreasing temperature does not involve Ca-rich pyroxene, as it does at lower pressures. Orthopyroxene, plagioclase, magnetite, and ilmenite appear almost simultaneously on the liquidus (920±5ºC at 200 MPa) of the 2004–6 dacite for H_2O-saturated conditions. Melt and phenocryst abundances were determined for representative experiments using the bulk-rock and melt compositions (table 5), along with phenocryst compositions from each experiment, in a mass-balance calculation (Wright and Doherty, 1971). Just within the amphibole stability field at 200 MPa (900ºC), the magma contains 8 weight percent crystals (4 percent plagioclase, 2 percent each of orthopyroxene and amphibole, and less than 1 percent of magnetite and ilmenite). At 850ºC and 200 MPa, the crystals make up 32 weight percent of the magma (M-27; table 4), and at 850ºC and 100 MPa, they make up 52 weight percent of the magma.

The composition of the plagioclase that is stable at any set of *P–T* conditions is contoured in figure 10 primarily on the basis of long-duration crystallization experiments, but reversals also were achieved. New-growth plagioclase is readily identifiable morphologically in higher temperature experiments (900±25ºC), and it was analyzed. Very long duration (15 to 30 days) crystallization experiments used a starting material created at 235 MPa to determine the stable plagioclase-composition contours at lower pressures, all at 850ºC. Plagioclase compositions used to create the contours in figure 10 are recorded in table 4.

The compositions of the amphibole produced are plotted in figure 11 for the experiments where new growth could be identified optically and in BSE images (table 6). Plotted for comparison are the data from representative natural phenocrysts in sample SH305. Six experiments run at 850ºC or 870ºC and pressures of 100–230 MPa all have amphiboles with 9–10.5 weight percent Al_2O_3, well outside the range observed in the normal cyclically zoned natural amphiboles (11.5–15 weight percent). The range of MgO (and FeO) in these low-temperature amphiboles is partly a function of the differences in f_{O_2} in this group of experiments, as illustrated by the most oxidized experi-

Table 4. Hydrothermal experiments on Mount St. Helens 2004 dacite.

[Total of 48 runs, arranged in order of decreasing pressure, from 260 to 70 MPa. Temperature ranges from 940ºC to 840ºC. Starting material was powder derived from sample SH305 (dome lava erupted November 2004) for 20 runs (shown as 305pdr); whereas starting material for other runs was product of an intervening run, shown listed. Oxygen fugacity buffered within 2 log units of nickel-nickel oxide (NNO). Crystallization products, listed in order of decreasing abundance (except glass), are plagioclase, Plg; amphibole; A; orthopyroxene, Opx; Cpx, clinopyroxene; magnetite, Mt; ilmenite, Il; and glass, L. Product listed in square brackets indicates phase is breaking down, is not in contact with melt, and is considered unstable at conditions of experiment; number in brackets refers to rim thickness on amphibole. Weight percent crystals shown parenthetically for some runs, determined by mass balance methods. Anorthite content of plagioclase, specified for 60 percent of runs, ranges from An_{71} to An_{34}.]

Run No.	Starting material	Pressure (MPa)	Temperature (ºC)	Buffer (Δ NNO)	Time (days)	Products	
M-45a	M-41	260	915	1	1.0	L	
M-63a	305pdr	260	850	-1	1.0	Plg, A, Opx, Mt, I, L	(25%)
M-63b	M-16	260	850	-1	1.0	An_{53}, A, Opx, Mt, I, L	(25%)
M-73	305pdr	250	895	0	1.5	Plg, A, Opx, Mt, I, L	
M-35	M-31	235	900	1	2	An_{68}, A, M, L	(3%)
M-20	305pdr	235	850	1	1.5	An_{50}, A, Opx, Mt, I, L	(32%)
M-49	M-17	225	860	1	5	An_{51}, Opx, A, Mt, L	
M-62	M-58+s	210	900	-1	2	An_{64}, Opx,A, Mt, L	
M-59a	M-56a	205	900	-2	1	An_{62}, A, Opx, Mt, L	
M-59b	M-19	205	900	-2	1	An_{62}, A, Opx, Mt, L	
M-60b	M-16	205	900	-2	1.5	Plg, A, Opx, Mt, L	
M-58	305pdr	200	930	1	1	L	
M-16	305pdr	200	922	1	2	Opx, Mt, [Plg], L	
M-24	305pdr	200	920	1	1.8	An_{71}, Opx, Mt, M, L	
M-19	M-17	200	915	1	0.5	Plg, Opx, M, L	(4%)
M-36	M-17	200	915	1	2	An_{70}, Opx, Mt, L	(2%)
M-41a	305pdr	200	910	1	2	An_{67}, Opx, A, Cpx, Mt, L	
M-41b	M-24	200	910	1	2	Plg, Opx, A, M, L	
M-50b	M-24	200	900	2	2	An_{62}, Opx, A, Mt, L	(8%)
M-51a	M-41a	200	900	-1	1	Plg, Opx, A, Mt, I, L	
M-51b	305pdr	200	900	-1	1	Plg, Opx, A, Mt, I, L	
M-56a	305pdr	200	900	-2	0.7	Plg, A, Opx, Mt, L	
M-25	M-24	200	885	1	2	An_{58}, A, Opx, Mt, I, L	
M-26	M-24	200	870	1	3	An_{52}, A, Opx, Mt, I, L	
M-66	305pdr	200	850	1	2	An_{42}, A, Opx, Mt, I, L	
M-27	M-24	200	850	1	6	An_{44}, A, Opx, Mt, I, L	
M-17	305pdr	200	840	1	4	Plg, A, Opx, Mt, I, L	
M-21	M-20	180	850	1	28	An_{40}, A, Opx, Mt, I, L	
M-48	M-34	150	905	1	2	Plg, A, Opx, Mt, I, L	
M-34	305pdr	150	880	1	2	An_{58}, A, Opx, Mt, I, L	
M-32	M-31	150	860	1	6	An_{42}, A, Opx, Mt, I, L	
M-28	M-24	150	860	1	6	Plg, A, Opx, Mt, I, L	
M-22	M-20	140	850	2	28	An_{37}, A, Opx, Mt, I, L	
M-54	305pdr	125	940	1	2	An_{70}, Opx, Mt, I, L	
M-44	M-39	125	930	1	3	An_{68}, Opx, Mt, I, L	
M-39	305pdr	125	920	1	1	An_{58}, A, Opx, Mt, I, L	
M-38	305pdr	125	910	1	2	An_{54}, Opx, Cpx, Mt, I, L	
M-31	305pdr	125	875	1	4	An_{44}, Opx, Cpx, [A], Mt, I, L	
M-46	M-30	125	864	1	6	An_{40}, A, Opx, Mt, I, L	
M-53	M-38	125	860	1	6	An_{39}, A, Opx, Mt, I, L	

Table 4. Hydrothermal experiments on Mount St. Helens 2004 dacite.—Continued

[Total of 48 runs, arranged in order of decreasing pressure, from 260 to 70 MPa. Temperature ranges from 940ºC to 840ºC. Starting material was powder derived from sample SH305 (dome lava erupted November 2004) for 20 runs (shown as 305pdr); whereas starting material for other runs was product of an intervening run, shown listed. Oxygen fugacity buffered within 2 log units of nickel-nickel oxide (NNO). Crystallization products, listed in order of decreasing abundance (except glass), are plagioclase, Plg; amphibole; A; orthopyroxene, Opx; Cpx, clinopyroxene; magnetite, Mt; ilmenite, Il; and glass, L. Product listed in square brackets indicates phase is breaking down, is not in contact with melt, and is considered unstable at conditions of experiment; number in brackets refers to rim thickness on amphibole. Weight percent crystals shown parenthetically for some runs, determined by mass balance methods. Anorthite content of plagioclase, specified for 60 percent of runs, ranges from An_{71} to An_{34}.]

Run No.	Starting material	Pressure (MPa)	Temperature (ºC)	Buffer (Δ NNO)	Time (days)	Products
M-54a	M-44	120	912	1	2.5	An_{56}, Opx, Cpx, Mt, I, L
M-54b	M-38	120	912	1	2.5	Plg, Opx, Cpx, Mt, I, L
M-52	305pdr	120	845	1	21	An_{56}, Opx, A, Mt, I, L (51 %)
M-47	305pdr	115	890	1	3	Plg, Opx, Cpx, Mt, I, L
M-30	305pdr	100	865	1	4	Plg, Opx, Cpx, Mt, I, [A, 8 μm], L
M-23	M-20	100	850	1	30	An_{34}, Opx, A, Mt, I, L
M-12	305pdr	82	850	1	10	Plg, Opx, Cpx, Mt, I, [A, 10 μm]
M-11	M-20	70	850	1	6	Plg, Opx, Cpx, Mt, I, [A, 8 μm]

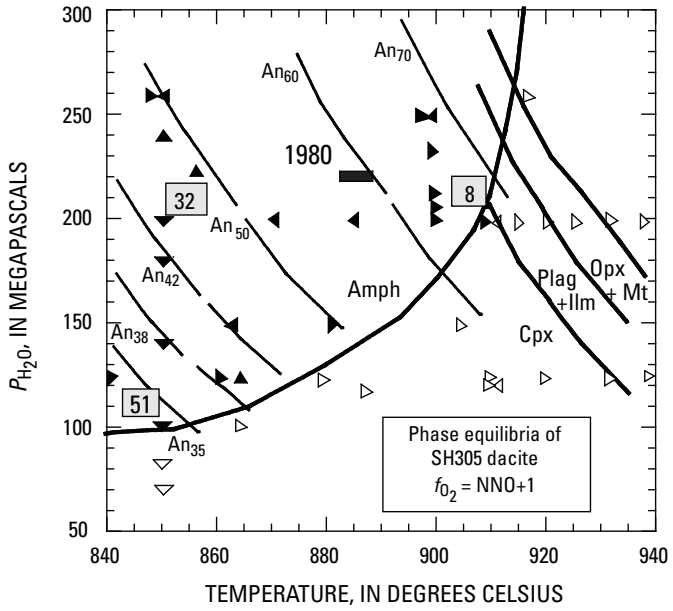

Figure 10. Pressure-temperature phase diagram determined for the Mount St. Helens 2004–6 dacite at water-saturated conditions and oxygen fugacity equal to NNO+1 log units. Symbols for individual experiments (table 4) point in the direction of approach to the final *P* and *T* plotted; solid symbols indicate amphibole is stable. Solid heavy lines mark upper stability limit for a given phenocryst phase: Cpx, Ca-pyroxene; Amph, amphibole; Plag, plagioclase; Opx, orthopyroxene; Mt, magnetite; Ilm, ilmenite. Medium-weight lines are contours labeled with plagioclase anorthite content (for example, An_{70}), on basis of data in table 4. Boxed numbers (8, 32, 51) indicate weight percent crystals present at *P*–*T* conditions occupied by box, as determined by a mass balance calculation (see text). Solid bar labeled 1980 shows estimated conditions in preeruption 1980 magma (Rutherford and others, 1985; Venezky and Rutherford, 1999).

Table 5. Bulk and experimental glass compositions, Mount St. Helens, Washington, 2004–2006.

[Chemical analyses determined by electron microprobe at Brown University, Providence, R.I.; J.D. Devine, analyst. Each analysis is an average; total number of analyses for each sample listed in row "Analyses." Compositions in weight percent; all Fe as FeO. Parenthetical numbers, standard deviation on average for the last places given. VBD, dissolved volatiles (H_2O) by difference. Column 1 (all glass), SH305 bulk composition.]

Sample ---	**SH-305**	**M-62**	**M-59a**	**M-51a**	**M-27**	**M-17**	**M-23**	**M-34**
T **(°C) ------**	**1300**	**900**	**900**	**900**	**850**	**850**	**850**	**890**
P **(MPa)---**	**0.1**	**210**	**205**	**200**	**200**	**200**	**100**	**150**
f_{O_2} **(ΔNNO)**	**+1**	**–1**	**–2**	**–1**	**+1**	**+1**	**+1**	**+1**
				Major-element analyses, weight percent				
SiO_2	64.80 (24)	62.48 (28)	62.48 (26)	61.59 (39)	65.30 (98)	67.69 (52)	72.83 (24)	67.95 (32)
TiO_2	0.64 (5)	0.60 (5)	0.54 (7)	0.52 (6)	0.32 (9)	0.25 (3)	0.25 (4)	0.34 (4)
Al_2O_3	17.23 (14)	15.85 (13)	15.94 (19)	16.06 (4)	14.46 (28)	13.91 (18)	12.38 (12)	13.68 (10)
FeO	4.35 (10)	3.24 (12)	3.22 (8)	3.15 (16)	2.10 (52)	2.11 (17)	1.42 (11)	2.40 (9)
MgO	1.91 (4)	1.26 (5)	1.24 (7)	1.45 (11)	0.68 (51)	0.46 (3)	0.21 (2)	0.53 (11)
CaO	4.68 (8)	3.93 (7)	3.93 (7)	4.28 (19)	1.96 (44)	2.13 (11)	1.20 (7)	2.27 (6)
Na_2O	4.58 (9)	4.84 (10)	4.84 (10)	4.64 (19)	5.60 (25)	4.77 (19)	4.60 (14)	4.66 (17)
K_2O	1.45 (7)	1.53 (6)	1.53 (6)	1.33 (11)	2.40 (14)	1.83 (9)	2.43 (11)	1.97 (4)
MnO	0.10 (3)	0.02 (3)	0.02 (3)	0.05 (2)	0.06 (5)	0.04 (3)	0.02 (4)	0.04 (3)
Total	99.74	93.75	93.68	93.07	92.89	93.19	95.34	93.84
Analyses	9	6	6	6	6	7	6	6
VBD	0	6.25	6.32	6.93	7.11	6.81	4.66	6.16

ment, M-22 (fig. 11*A*). The externally imposed f_{O_2} in the 900ºC experiments ranges from 2 log units below to 2 log units above NNO, bracketing the f_{O_2} indicated by the Fe-Ti oxides (NNO +1) in the natural sample.

The variation in Al_2O_3 content (including Al_{total} and ^{VI}Al) of amphibole that crystallizes from the 2004–6 dacite (table 6) should be a function of temperature and pressure as discussed earlier in this paper, and the experimental data (fig. 11) show this to be the case. It is notable, however, that only experiments done at 200 MPa and higher pressures have compositions that plot in the zone defined by the cyclically zoned natural phenocrysts. Additionally, none of the experiments in the pressure range 200–250 MPa produced amphiboles comparable to the highest Al- and Fe-rich zones in the natural amphibole. Experiments at 200 MPa, 900ºC, and a log f_{O_2} in the range NNO+2 to NNO-2 produce the low and intermediate Al_2O_3 compositions in the cyclically zoned natural phenocrysts. Experiments at 900ºC and pressures of 235 MPa (NNO+1) and 250 MPa using the NNO buffer did not produce an amphibole with higher Al. Both the Al_2O_3 and ^{VI}Al composition data indicate that a pressure somewhat greater than 250 MPa is required to stabilize the highest Al- and Fe-rich amphibole end members of the natural phenocrysts.

Depth of the Preeruptive 2004–2006 Magma System

The question of preeruptive magma-storage depth is of considerable interest and importance for understanding the ongoing Mount St. Helens eruption and for predicting how the eruption is likely to progress. Is the magma erupting from the same storage zone determined for the 1980–86 eruptions (Scandone and Malone, 1985; Rutherford and others, 1985), or has the system changed? The seismic record over the decade before the new eruption suggests that magma may have moved to a relatively shallow depth (3–4 km) below the crater floor, particularly at one or two times during this period (Moran, 1994; Moran and others, this volume, chap. 2). Seismicity accompanying the 2004 eruption appears to have been largely in the region from 2 km to the surface, consistent with magma erupting from storage below this depth. Theoretically, the abundance and composition of phenocrysts, particularly the rim compositions, are dependent on the final *P* and *T* of phenocryst-melt equilibration in the erupting magma. We have attempted to use this knowledge and the phenocryst data from the natural sample and experiments to determine the depth of the magma storage upper boundary.

As described in the previous section, most of the amphibole-phenocryst growth in the 2004–6 dacite was at pressures of 200 MPa or higher and at temperatures greater than 850ºC. The phenocryst abundance in the dacite at these high pressures is less than 32 volume percent at temperatures greater than 850ºC (fig. 10). However, given that much of the magma erupted at 850ºC with ~45 volume percent phenocrysts (Pallister and others, this volume, chap. 30), plagioclase phenocryst growth must have continued to a much lower pressure (fig. 10). Analytical data from experiments designed to achieve a good approach to plagioclase phenocryst rim-melt equilibrium as a function of pressure at 850ºC are compared with rim-composition measurements in the natural samples (figure 12).

Table 6. Representative experimental amphibole compositions and structure formulas, Mount St. Helens, Washington, 2004–2006.

[Chemical analyses determined by electron microprobe at Brown University, Providence, R.I.; J.D. Devine, analyst. Compositions in weight percent; all Fe as FeO. Structure formula calculated after Holland and Blundy (1994). Magnesium number, Mg# = (Mg×100)/(Mg+(Fe^{2+} in Y site)).]

Sample No.---	**M-62**	**M-59b**	**M-59a**	**M-51a**	**M-49**
***P* (MPa)-------**	**210**	**205**	**205**	**200**	**225**
***T* (°C)----------**	**900**	**900**	**900**	**900**	**860**
f_{O_2} (ΔNNO)--	**-1**	**-2**	**-2**	**-1**	**1**
Major-element analyses, weight percent					
SiO_2	42.63	43.68	43.58	42.07	44.44
TiO_2	2.48	2.28	2.62	2.72	1.89
Al_2O_3	13.38	12.54	11.31	13.00	10.31
FeO	13.13	10.72	11.48	14.07	14.95
MgO	13.30	15.21	14.90	13.14	13.15
CaO	10.95	11.07	11.06	11.58	10.56
Na_2O	2.25	2.37	2.26	2.39	1.89
K_2O	0.27	0.33	0.26	0.32	0.26
MnO	0.19	0.11	0.21	0.10	0.26
Total	98.58	98.31	97.68	99.39	97.71
Cation abundance in structure formula					
Si	6.119	6.224	6.275	6.041	6.452
Al^{IV}	1.881	1.776	1.725	1.959	1.548
Ti	0.268	0.244	0.284	0.294	0.206
Al^{VI}	0.383	0.331	0.195	0.241	0.216
Fe^{3+}	0.728	0.654	0.701	0.745	0.823
Fe^{2+}(Y)	0.776	0.536	0.622	0.908	0.909
Mg	2.846	3.231	3.198	2.812	2.846
Ca	1.684	1.690	1.706	1.782	1.643
Fe^{2+}(X)	0.072	0.088	0.059	0.037	0.083
Na	0.627	0.609	0.631	0.665	0.532
Mg#	78.57	85.78	83.71	75.60	75.80
$Fe^{3+}/\Sigma Fe$	0.462	0.512	0.507	0.441	0.454

Sample No.---	**M-32**	**M-28**	**M-20**	**M-27**	**M-22**
***P* (MPa)-------**	**150**	**150**	**234**	**200**	**140**
***T* (°C)----------**	**200**	**860**	**850**	**850**	**850**
f_{O_2} (ΔNNO)--	**1**	**1**	**1**	**1**	**1**
Major-element analyses, weight percent					
SiO_2	44.72	45.19	45.59	42.92	46.04
TiO_2	2.46	1.73	1.68	2.14	1.49
Al_2O_3	9.29	10.26	9.48	11.49	8.58
FeO	14.58	13.12	14.21	15.80	11.60
MgO	13.07	14.04	13.71	12.19	15.48
CaO	11.14	11.28	11.32	10.97	11.36
Na_2O	1.97	1.98	1.79	2.23	1.94
K_2O	0.27	0.28	0.26	0.32	0.24
MnO	0.14	0.18	0.28	0.21	0.29
Total	97.64	98.06	98.32	98.27	97.02
Cation abundance in structure formula					
Si	6.540	6.515	6.575	6.264	6.659
Al^{IV}	1.460	1.485	1.425	1.736	1.341
Ti	0.271	0.188	0.182	0.235	0.162
Al^{VI}	0.141	0.259	0.187	0.240	0.121
Fe^{3+}	0.558	0.625	0.698	0.745	0.670
Fe^{2+}(Y)	1.182	0.911	0.986	1.129	0.709
Mg	2.849	3.017	2.947	2.652	3.337
Ca	1.745	1.77	1.749	1.715	1.761
Fe^{2+}(X)	0.043	0.046	0.030	0.055	0.024
Na	0.558	0.554	0.500	0.631	0.542
Mg#	70.68	76.81	74.93	70.14	82.47
$Fe^{3+}/\Sigma Fe0$	0.313	0.395	0.407	0.386	0.478

The results of the plagioclase-growth experiments indicate that if the 2004–6 magma was stored for more than 30 days at 180 MPa before experiencing a fairly rapid ascent to the surface, the rim compositions would be approximately An_{40}. The similarity of the 14- and 28-day experimental results suggest that much longer storage at this depth would not change the most albite-rich composition observed, as long as the temperature and P_{H_2O} remained unchanged. At 140 and 100 MPa, the plagioclase in equilibrium with the residual melt at 850ºC is An_{35} and An_{32}, respectively. Comparing these experimental plagioclase compositions to the most Na-rich rims on natural phenocrysts in SH304 and SH305 suggests that the phenocrysts in the 2004–6 magma were crystallizing at a pressure as low as 120–140 MPa before the final ascent. The natural phenocrysts with more Ca-rich rims (fig. 12) are interpreted to have experienced little or no growth in the decompression accompanying ascent to 120 MPa. This lack of new plagioclase growth is expected in an ascending magma when the phenocryst content is high, because the melt immediately adjacent to some phenocrysts is limited in volume by other phenocrysts that are close or touching. Additionally, because the ascent from the storage zone to the surface did not produce significant reaction rims on amphiboles, we conclude that measurable additions to the plagioclase phenocrysts are unlikely to be added during the final (100 to 0.1 MPa) ascent. We make this conclusion because H_2O loss from the melt in ascending magma is the main cause of both amphibole breakdown and plagioclase crystallization. The amphibole rims are less than 5 μm thick in these samples, indicating a relatively rapid magma ascent (Rutherford and Hill, 1993; Rutherford and Devine, 2003). Although nucleation and growth of plagioclase microlites occurs readily in such decompressions (Geschwind and Rutherford, 1995), the experimental data indicate that additions to associated phenocrysts would be minor and too thin to analyze by electron microprobe.

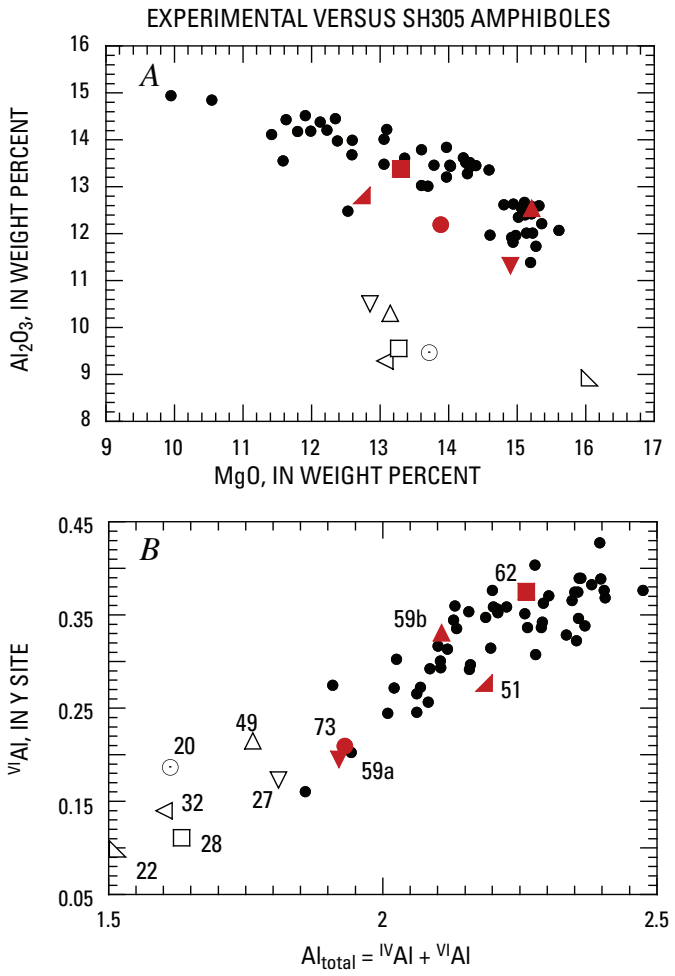

Figure 11. Compositions of amphiboles produced in hydrothermal experiments (table 4) compared with those of natural cyclically zoned phenocrysts in SH305, a representative phenocryst in 2004–6 magma. Black solid dots, natural amphiboles; open symbols, experimental results at temperatures from 840ºC to 870ºC and pressures less than 200 MPa. Solid red symbols represent experiments at 900ºC and pressures of 200–260 MPa. The f_{O_2} of the 900ºC experiments ranged from NNO-2 to NNO+2; others were all at NNO+1 log units. Numbered symbols indicate amphibole compositions (table 6) produced in experiments; numbers correspond to sample numbers in table 4. *A*, Al_2O_3 versus MgO. *B*, ^{VI}Al versus Al_{total}.

To summarize, the plagioclase rim compositional data indicate that the 2004–6 magma could have been stored at a pressure as low as 120 MPa, or a depth of 4–5 km below the crater floor for a relatively prolonged period before eruption. When these data are considered together with the depth range indicated by seismic data during the eruption (Moran and others, this volume, chap. 2), the 4–5-km depth appears to represent the top of the magma storage zone. However, it is also obvious that the preeruptive magma storage extended to much greater depths, and the Na-rich plagioclase phenocryst rims may have developed during the slow, final ascent process that began somewhere below 4 km.

The amphibole phenocryst compositions and their very thin decompression-induced reaction rims do not significantly constrain estimates of the preeruptive magma storage-zone depth, except to indicate that it was greater than 100 MPa (4–5 km) for magma at 850ºC. If the storage zone pressure had been less than 100 MPa, there would have been thick, coarse-grained reaction rims on all amphiboles. For example, 10-μm-thick rims were produced in experiments at 85 and 70 MPa on the 2004–6 dacite in as little as 7 days (experiments M-11 and M-12; table 4). However, as discussed in the following section, the crystallization of the cyclically zoned amphiboles must have occurred at pressures more than twice the 100 MPa estimated for the final pressure of phenocryst-melt equilibration. No attempt was made to use the Al-in-hornblende geobarometer to estimate the pressure because the phenocryst phase assemblage in the 2004–6 dacite is not silica saturated as required by the geobarometer calibration (Johnson and Rutherford, 1989). Using the geobarometer (Thornber and others, this volume, chap. 32) should give an upper-pressure limit, particularly for the early crystallization of the Al-rich amphiboles.

Origin of the Cyclically Zoned Phenocrysts: Preeruptive Magma History

A second objective of this project was to determine the origin and significance of the cyclic compositional zonation observed in 2004–6 magma phenocrysts. Is it possible to crystallize the cyclically zoned plagioclase, amphibole, and orthopyroxene phenocrysts by simply changing conditions in the dacite magma, or are injections of mafic magma required? For example, the presence of cyclically zoned phenocrysts in the silicic andesite magma erupted recently (1995–2002) at Soufrière Hills, Montserrat, was clearly the result of recrystallization following injections of a more mafic basaltic andesite (Rutherford and Devine, 2003). Vesicular blobs of the mafic magma were carried up in the erupting magma, and small, blade-shaped crystals of high-An plagioclase and pargasitic amphibole from the mafic magma are present in the andesite groundmass. However, there is no evidence of recent mafic magma injections into the 2004–6 dacite (Pallister and others, this volume, chap. 30). Thus, we have concentrated on determining how the 2004–6 phenocryst compositions could have been formed from dacite magma by trying to determine the range of pressure-temperature conditions where the various phenocryst compositions would crystallize.

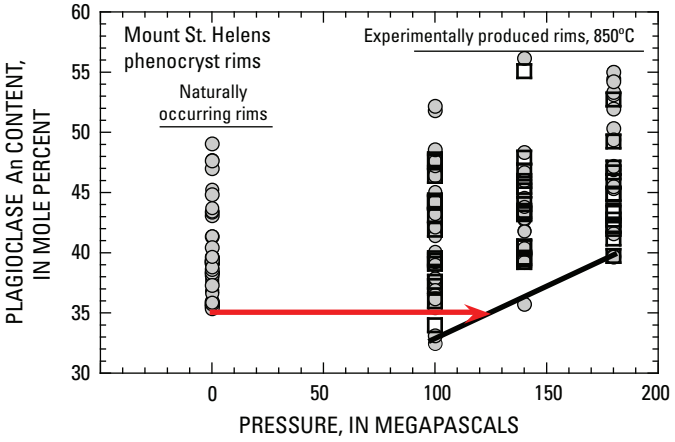

Figure 12. Comparison of plagioclase phenocryst-rim compositions in samples from 2004–2006 Mount St. Helens eruption (SH304 and SH305) with those produced in long-duration crystallization experiments at 850°C and pressures of 100 to 180 MPa (table 4). Squares, 15-day runs; circles, 30-day runs. Similarity between different run durations indicates experiments were sufficiently long to approach chemical equilibrium. Arrow indicates pressure (about 120 MPa) where these experiments produce new plagioclase that is compositionally equal to most Na-rich rims on the natural phenocrysts. More Ca-rich rims in natural plagioclase are interpreted as rims where there was limited late-stage growth.

Figure 13 is a model of the Mount St. Helens 2004–6 magma storage zone that uses the experimental data described above to explain the cyclic zoning of the natural amphibole, plagioclase, and orthopyroxene phenocrysts. Because there is no evidence, such as mafic enclaves, to indicate other magma compositions were mixed or mingled with the 2004–6 dacite, our model assumes a dacite magma input. The timing of this input is not known; it could have been associated with the beginning stages of the 2004–6 eruption, or it could have been associated with past (1986–98) peaks in deep seismic activity (Moran and others, this volume, chap. 2). Given that the preeruptive magmatic temperatures decreased from 1980 to 1986 (Rutherford and Hill, 1993), it seems unlikely that the hot 2004–6 magma was emplaced during the 1980–86 eruptions, although this possibility cannot be ruled out. The homogeneity of the 2004–6 dacite suggests that the magma composition entering the base of the storage zone is similar to the magma that has been erupting. Uranium-series dating of mineral separates from the 2004–6 magma indicate there is an old component present in the erupting magma (Cooper and others, this volume, chap. 36), but this may be explained by the xenolithic material, and it does not appear to affect our conclusions about magma entering the 2004–6 system.

If the incoming dacite magma had a high dissolved water content, as the phenocryst phase assemblage suggests, it would crystallize Fe- and Al-rich amphibole before or during its invasion of the storage zone at about 900ºC (fig. 13). This temperature for the incoming magma is suggested by the high-TiO_2 magnetite phenocrysts in some of the samples (fig. 9), by the lack of plagioclase inclusions in amphibole phenocrysts that indicate that amphibole crystallized before plagioclase, and by the anorthite content (An_{68}) in the cores of cyclically zoned plagioclase phenocrysts. Small amounts of orthopyroxene, magnetite, and ilmenite crystallized along with the early amphibole as indicated by inclusions in amphibole and the experimental phase equilibria. The pressure on the magma as it enters the storage zone is interpreted to be ~300 MPa (12 km depth) on the basis of the experiments (fig. 11) that indicate such pressures are required to stabilize the high-Al zones in the amphibole phenocrysts. Importantly, An_{68} plagioclase is not stable above 200 MPa at 880–900ºC, according to the water-saturated experiments (fig. 10), and would be lacking in the phenocryst-poor magma just after it entered the storage zone.

As the water-rich magma moved higher in the storage zone, the high-An (An_{68}) zones in plagioclase would begin to crystallize at 200 MPa and temperatures near 900ºC. At this point (about 7–8 km depth), much of the magma must stagnate and cool in the storage zone in order to form the more Ab-rich zones in the plagioclase and the more Mg-rich zones in the amphiboles. The plagioclase phenocrysts require that the magma cools to 850ºC in order to stabilize and grow the albite-rich layer ($An_{45–50}$) in the first growth cycle. We interpret this cooling as occurring in a lateral flow (fig. 13). If cooling did not occur, the original phenocrysts would tend to dissolve during convection to depth, and textures within phenocrysts indicate dissolution was not extensive. The second cycle of

amphibole growth begins with an Fe- and Al-rich material that is stable only at pressures substantially greater than 200 MPa (fig. 11); the amphibole data require the convection system shown in figure 13. Sharp chemical transitions—those between Na-rich and Na-poor zones in plagioclase (200 MPa and 850ºC) and those between Mg-rich and Fe-rich zones in amphibole—are consistent with the convection process, in that crystallization would not occur in the sinking magma.

The forces to drive the convection certainly are present. The melt-rich character, relatively high temperature, and high dissolved H_2O content would tend to make the incoming magma buoyant in the storage zone occupied by older, cooler, and more crystal-rich magma. During ascent from the 12-km depth, the buoyancy of this magma would decrease as a result of decompression-induced crystallization. Cooling, crystallization, and loss of released gas at the top of the convective cell would further reduce the buoyancy of the magma, apparently to the point where the combination of density and viscosity cause it to sink in the chamber. Using the data of Geschwind and Rutherford (1995) for the densities of the phases, the density of the magma would increase from 2,310 kg/m^3, as magma with 5 volume percent crystals (amphibole and orthopyroxene) enters the storage zone, to 2,450 kg/m^3 at 850ºC where magma contains 30 volume percent phenocrysts

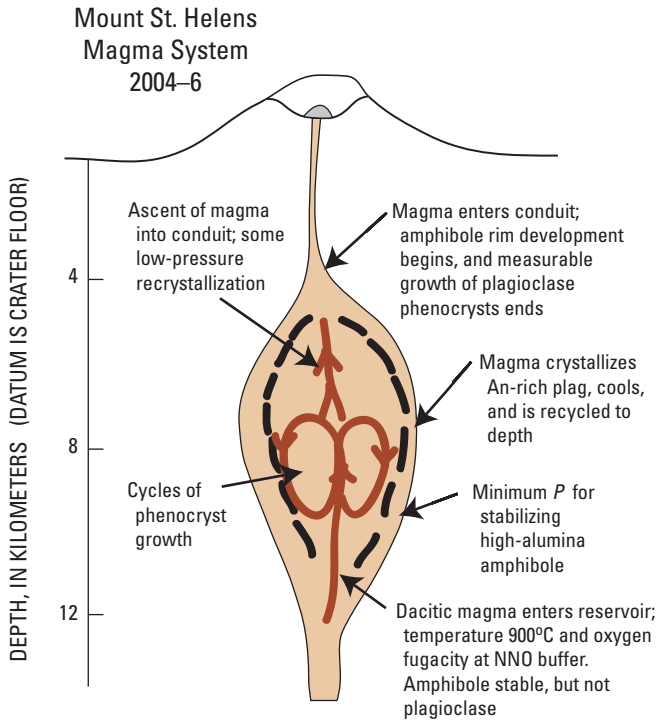

Figure 13. Simplified cross section showing model of the Mount St. Helens magma storage zone and transport system based on petrologic data for the 2004–6 samples discussed in this paper (see also Pallister and others, this volume, chap. 30) and the seismic depths associated with magma movement before and during the 2004 eruption (Moran and others, this volume, chap. 2). Depth scale is relative to the crater floor.

(in the proportions plag:amph:opx:mt = 23:3:3:1 on a volume percent basis). This represents a 6-percent density increase of the crystal-rich magma relative to the incoming melt-rich magma, assuming gas released in the upwelling process is able to escape during the crystallization. Given that viscosity of the H_2O-rich melt will be relatively low, the viscosity of the phenocryst-poor magmas should facilitate the convection. Sharp increases in viscosity when the phenocryst content goes above 30 volume percent (Marsh, 1981) may indicate why the cycle ends and why there are only two zoning cycles, on average, in amphibole.

Following an average of two cycles of phenocryst growth and convective overturn, some fraction of the magma would separate and rise toward the conduit. Although there were additions to the plagioclase phenocrysts in this stage of magma ascent (fig. 12), there was almost no additional amphibole crystallization, because the interstitial H_2O-saturated melt at 200 MPa and 850ºC has essentially no amphibole component, and there is no Ca-rich pyroxene in the H_2O-rich dacite. However, amphibole recrystallization to form Fe-rich, Al-poor amphibole rims, as observed in SH323 (fig. 7) may occur in magma that spent a somewhat longer-than-average time in the less-than-200-MPa pressure range during this ascent.

A variation of the above model involving an incoming magma that has a somewhat lower initial dissolved H_2O content cannot be ruled out. Rather than H_2O-saturated, the incoming magma could have a P_{H_2O} as low as 0.7 P_{total}, in which case the amphibole stability would not have been affected, but plagioclase phenocrysts would have been stabilized to a higher temperature at a given pressure. This is equivalent to proposing that the magma was saturated with a CO_2-bearing fluid when it entered the storage zone. As discussed above, however, the initial melt-rich magma must have contained at least 4 weight percent dissolved H_2O in order to stabilize amphibole, and this limits the CO_2 content of the coexisting fluid (Newman and Lowenstern, 2002) to ~600 ppm. The maximum temperature of the magma coming into the storage zone at 260–300 MPa is still required to be less than 910ºC in order to stabilize the high-Al amphibole. However, in this case, the An_{68} plagioclase cores could have formed at pressures greater than 200 MPa, possibly as early as the amphibole. The absence of plagioclase inclusions in the amphibole cores suggests this variant of the storage zone model is unlikely.

Comparison of 2004–2006 and 1980–1986 Preeruption Magmas

Some additional data collected for the 1986 lava dome (sample SH205) and for the 1980 pumice (SH084) during the course of this study indicate that a set of convective processes similar to those described above was operating in the magma storage zone during the 1980–86 eruptions. Magma

erupted in 1986 last equilibrated at 860±10ºC (Rutherford and Hill, 1993) and contained amphiboles with cyclic zoning generally indistinguishable from that in the 2004–6 magma. A plot of Al_2O_3 versus MgO for amphiboles (fig. 14) shows essentially total overlap between typical amphiboles from SH205 (1986) and SH323 (2005; table 2 and fig. 4). A cyclical set of phenocryst growth conditions similar to that outlined for the 2004–6 magmas (fig. 13) appears to be required for the 1986 dome-forming lava. The lack of decompression-induced rims on amphibole in the 1986 sample (fig. 3*D*) is one significant example of how the 1986 magma differs from that erupted in 2004–6. This observation seems to require an even more rapid ascent for the 1986 magma over the final 4–5 km. Outer rims on the 1986 amphibole that are higher in FeO, relative to those in the 2004–6 magma, might also be explained by a rapid ascent of magma from depth. This mineralogical evidence of amphibole crystallization over a pressure range suggests a process similar to one proposed recently (Blundy and Cashman, 2005; Cashman and McConnell, 2005) as operating in the Mount St. Helens magma system, on the basis of melt-inclusion data. The magma ascent history, however, appears to have been more complicated than can be determined from the melt inclusions.

Compositional zoning in representative amphibole phenocrysts from the May 18, 1980, white pumice is shown in figure 14. The Al_2O_3 versus MgO zoning within individual 1980 phenocrysts defines line segments that are parallel to the 2004–6 trend, but they range down to significantly lower Al_2O_3. The lower-Al_2O_3 phenocrysts are similar in composition to the Al-poor rims analyzed on amphiboles in SH323 (fig. 7) and other more recently erupted 2004–6 samples. In a previous section we suggested that the composition of the anomalous Al-poor rims on SH323 amphiboles are best explained by recrystallization at pressures of 100–200 MPa, possibly even just outside (below) the stability limit of OH-amphibole. This would help explain the fluorine enrichment of these rim compositions. These observations suggest that the convective process described in the model for the 2004–6 magma storage zone also was working in 1986 and 1980. However, at least some of the 1980 magma seems to have experienced a significant part of the amphibole crystallization at a pressure in the 150–200 MPa range at the 880ºC temperature (Rutherford and Devine, 1988; Venezky and Rutherford, 1999) of this system. The 1980 phenocrysts generally are higher in F (~1,200 ppm) than are the cores of 2004–6 samples (900 ppm) but are not as high as the 2004–6 rims (SH323), consistent with this lower-pressure origin.

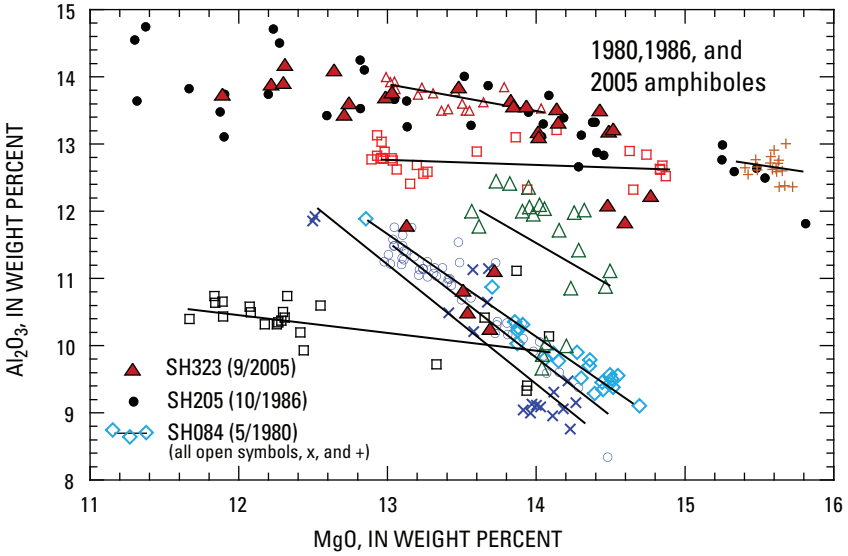

Figure 14. Compositions of eight amphibole phenocrysts (rim to rim transects) in the 1980 Mount St. Helens pumice (SH084) compared with similar amphibole transects for a typical sample of the 2004–6 lava dome (SH323) and 1986 dome (SH205). Lines are fit to the eight SH084 amphibole profiles. Zoning in the 1980 pumice phenocrysts is similar to that in the 2004–6 phenocrysts except that it occurs at lower Al_2O_3 in most crystals. Note that rims on SH323 amphiboles spread over the low-Al_2O_3 compositions found in the May 1980 samples, whereas the zoning profile in SH205 (1986 lava) is indistinguishable from 2004–6 samples such as SH304 and SH305 (fig. 4).

Conclusions

In summary, and in answer to the questions posed in the introduction to this paper, the following conclusions can be made: (1) The phenocryst assemblage that occurs in the 2004–6 Mount St. Helens dacite lava-dome samples can be attributed to crystallization from dacite magma; no mafic magma injection is required. (2) The compositions of the Fe-Ti oxides, magnetite and ilmenite, although somewhat variable, indicate that the temperature of equilibration was in the range of 820–890ºC and the f_{O_2} was NNO + 1 log unit. The existence of a range of TiO_2 in different, relatively homogenous titanomagnetite phenocrysts also suggests there was mingling of different batches of dacite with different thermal histories to create each batch of erupting magma. (3) Cyclic zoning observed in amphiboles in the 2004–6 magma consists of Al- and Fe-rich zones alternating with Mg- and Si-rich zones and can be explained as approximately equal amounts of two substitutions: a pressure-sensitive Al-Tschermak substitution and a temperature-controlled edenite substitution. Significantly, different amounts of the Al-Tschermak end member, in different zones of each amphibole phenocryst, require crystallization over a range of total pressure. Hydrothermal experiments on the dacite composition show that the Fe- and Al-rich end member of the amphibole zoning must have crystallized at pressures of ~300 MPa, whereas more Mg- and Si-rich amphibole zones crystallized in the 200-MPa range. (4) Cyclical zoning in natural plagioclase phenocrysts, ranging from An_{68} to An_{35}, also requires the magma to cycle through a range of crystallization conditions. The hydrothermal experiments indicate that An_{68} plagioclase would crystallize at ~200 MPa and 900ºC, well after the initial crystallization of amphibole in an ascending dacite magma. Cooling to ~850ºC is required to develop the first layer of Ab-rich plagioclase. (5) In order to explain the cyclic zoning in the phenocrysts, each batch of magma must have experienced convective overturn, going back to near the original high pressure at the lower temperature (850ºC), where it interacted with new incoming dacite magma, as illustrated in figure 13. (6) Rims on plagioclase phenocrysts, as sodic as An_{35}, indicate that plagioclase phenocryst growth continued in ascending magma until the pressure was ~130 MPa. This pressure is interpreted to represent the top of the magma storage zone at 4–5 km depth. (7) Compositional zoning in the 1980 and 1986 amphibole phenocrysts indicates that convective conditions also existed during phenocryst growth in that magma system.

Acknowledgments

We acknowledge the financial support of the National Science Foundation and field support from the Cascades Volcano Observatory staff for providing samples. We thank the members of the Mount St. Helens petrology working group for assistance and ideas and for providing access to manuscripts during their preparation. Finally, we acknowledge productive discussions with John Pallister and Carl Thornber and insightful reviews by Jon Blundy and Wes Hildreth.

References Cited

Andersen, D.J., and Lindsley, D.H., 1988, Internally consistent solution models for Fe-Mg-Mn-Ti oxides: Fe-Ti oxides: American Mineralogist, v. 73, nos. 7–8, p. 714–726.

Andersen, D.J., Lindsley, D.H., and Davidson, P.M., 1993, QUILF; a Pascal program to assess equilibria among Fe-Mg-Mn-Ti oxides, pyroxenes, olivine, and quartz: Computers and Geosciences, v. 19, p. 1333–1350.

Bachmann, O., and Dungan, M.A., 2002, Temperature-induced Al-zoning in hornblendes of the Fish Canyon magma, Colorado: American Mineralogist, v. 87, p. 1062–1076.

Blundy, J., and Cashman, K., 2005, Rapid decompression-driven crystallization recorded by melt inclusions from Mount St. Helens volcano: Geology, v. 33, no. 10, p. 793–796, doi:10.1130/G21668.1.

Cashman, K.V., and McConnell, S.M., 2005, Multiple levels of magma storage during the 1980 summer eruptions of Mount St. Helens, WA: Bulletin of Volcanology, v. 68, no. 1, p. 57–75, doi:10.1007/s00445-005-0422-x.

Cooper, K.M., and Donnelly, C.T., 2008, ^{238}U-^{230}Th-^{226}Ra disequilibria in dacite and plagioclase from the 2004–2005 eruption of Mount St. Helens, chap. 36 *of* Sherrod, D.R., Scott, W.E., and Stauffer, P.H., eds., A volcano rekindled; the renewed eruption of Mount St. Helens, 2004–2006: U.S. Geological Survey Professional Paper 1750 (this volume).

Cosca, M.A., Essene, E.J., and Bowman, J.R., 1991, Complete chemical analyses of metamorphic hornblendes; implications for normalizations, calculated H_2O activities, and thermobarometry: Contributions to Mineralogy and Petrology, v. 108, p. 472–484.

Devine, J.D., Rutherford, M.J., Norton, G.E., and Young, S.R., 2003, Magma storage region processes inferred from geochemistry of Fe-Ti oxides in andesitic magma, Soufrière Hills volcano, Montserrat, W.I.: Journal of Petrology, v. 44, no. 8, p. 1375–1400, doi:10.1093/petrology/44.8.1375.

Garcia, M.O., and Jacobson, S.S., 1979, Crystal clots, amphibole fraction, and the evolution of calc-alkaline magmas: Contributions to Mineralogy and Petrology, v. 69, p. 319–327.

Geschwind, C.-H., and Rutherford, M.J., 1995, Crystallization of microlites during magma ascent; the fluid mechanics of 1980–1986 eruptions at Mount St. Helens: Bulletin of Volcanology, v. 57, no. 5, p. 356–370.

Heliker, C., 1995, Inclusions in Mount St. Helens dacite erupted from 1980 through 1983: Journal of Volcanology and Geothermal Research, v. 66, nos. 1–4, p. 115–135, doi:10.1016/0377-0273(94)00074-Q.

Holland, T., and Blundy, J., 1994, Non-ideal interactions in calcic amphiboles and their bearing on amphibole-plagioclase thermometry: Contributions to Mineralogy and Petrology, v. 116, no. 4, p. 433–447, doi:10.1007/BF00310910.

Johnson, M.C., and Rutherford, M.J., 1989, Experimental calibration of the Al-in-hornblende geobarometer with application to the Long valley caldera (California) volcanic rocks: Geology, v. 17, p. 837–841.

Marsh, B.D., 1981, On the crystallinity, probability of occurrence, and rheology of lava and magma: Contributions to Mineralogy and Petrology, v. 78, p. 85–98.

Mastin, L.G., 1994, Explosive tephra emissions at Mount St. Helens, 1989–1991; the violent escape of magmatic gas following storms?: Geological Society of America Bulletin, v. 106, no. 2, p. 175–185.

Merzbacher, C., and Eggler, D.H., 1984, A magmatic geohygrometer; application to Mount St. Helens and other dacitic magmas: Geology, v. 12, p. 587–590.

Moran, S.C., 1994, Seismicity at Mount St. Helens, 1987–1992; evidence for repressurization of an active magmatic system: Journal of Geophysical Research, v. 90, no. B3, p. 4341–4354, doi:10.1029/93JB02993.

Moran, S.C., Malone, S.D., Qamar, A.I., Thelen, W.A., Wright, A.K., and Caplan-Auerbach, J., 2008, Seismicity associated with renewed dome building at Mount St. Helens, 2004–2005, chap. 2 *of* Sherrod, D.R., Scott, W.E., and Stauffer, P.H., eds., A volcano rekindled; the renewed eruption of Mount St. Helens, 2004–2006: U.S. Geological Survey Professional Paper 1750 (this volume).

Nakamura, M., 1995, Continuous mixing of crystal mush and replenished magma in the ongoing Unzen eruption: Geology, v. 23, p. 807–810.

Newman, S., and Lowenstern, J.B., 2002, Volatilecalc; a silicate melt-H_2O-CO_2 solution model written in Visual Basic for exel®: Computers and Geosciences, v. 28, no. 5, p. 597–604, doi:10.1016/S0098-3004(01)00081-4.

Pallister, J.S., and Thornber, C.R., 2005, Is the 2004–05 eruption of Mount St. Helens tapping new dacite from the deep crust? [abs.]: Eos (American Geophysical Union Transactions), v. 86, no. 52, Fall Meeting Supplement, Abstract V52B–05.

Pallister, J.S., Thornber, C.R., Cashman, K.V., Clynne, M.A., Lowers, H.A., Mandeville, C.W., Brownfield, I.K., and Meeker, G.P., 2008, Petrology of the 2004–2006 Mount St. Helens lava dome—implications for magmatic plumbing and eruption triggering, chap. 30 *of* Sherrod, D.R., Scott, W.E., and Stauffer, P.H., eds., A volcano rekindled; the renewed eruption of Mount St. Helens, 2004–2006: U.S. Geological Survey Professional Paper 1750 (this volume).

Rutherford, M.J., and Devine, J.D., 1988, The May 18, 1980, eruption of Mount St. Helens, III; stability and chemistry of amphibole in the magma chamber: Journal of Geophysical Research, v. 93, no. B10, p. 11949–11959.

Rutherford, M.J., and Devine, J.D., 2003, Magmatic conditions and magma ascent as indicated by hornblende phase equilibria and reactions in the 1995–2002 Soufrière Hills magma: Journal of Petrology, v. 44, p. 1433–1454.

Rutherford, M.J., and Devine, J.D., 2005, Crystallization of and conditions in the MSH 2004–05 dacite magma as indicated by phenocryst compositions and experiments [abs]: Eos (American Geophysical Union Transactions), v. 86, no. 52, Fall Meeting Supplement, Abstract V52B–05.

Rutherford, M.J., and Hill, P.M., 1993, Magma ascent rates from amphibole breakdown; an experimental study applied to the 1980–1986 Mount St. Helens eruptions: Journal of Geophysical Research, v. 98, no. B11, p. 19667–19685.

Rutherford, M.J., Sigurdsson, H., Carey, S., and Davis, A., 1985, The May 18, 1980, eruption of Mount St. Helens, 1; melt composition and experimental phase equilibria: Journal of Geophysical Research, v. 90, no. B4, p. 2929–2947.

Scandone, R., and Malone, S.D., 1985, Magma supply, magma discharge and readjustment of the feeding system of Mount St. Helens during 1980: Journal of Volcanology and Geothermal Research, v. 23, nos. 3–4, p. 239–262, doi:10.1016/0377-0273(85)90036-8.

Thornber, C.R., Pallister, J.S., Lowers, H.A., Rowe, M.C., Mandeville, C.W., and Meeker, G.P., 2008, Chemistry, mineralogy, and petrology of amphibole in Mount St. Helens 2004–2006 dacite, chap. 32 *of* Sherrod, D.R., Scott, W.E., and Stauffer, P.H., eds., A volcano rekindled; the renewed eruption of Mount St. Helens, 2004–2006: U.S. Geological Survey Professional Paper 1750 (this volume).

Venezky, D.Y., and Rutherford, M.J., 1999, Petrology and Fe-Ti oxide reequilibration of the 1991 Mount Unzen mixed magma: Journal of Volcanology and Geothermal Research, v. 89, p. 213–230, doi:10.1016/S0377-0273(98)00133-4.

Wallace, P.J., 2005, Volatiles in subduction zone magmas; concentrations and fluxes based on melt inclusion and volcanic gas data: Journal of Volcanology and Geothermal Research, v. 140, nos. 1–4, p. 217–240, doi:10.1016/j.jvolgeores.2004.07.023.

Wright, T.L., and Doherty, P.C., 1971, A linear programming and least squares method for solving petrologic mixing problems: Geological Society of America Bulletin, v. 81, p. 1995–2008.